

Chiroptical and Colorimetric Switches Based on Helical Polymer-Metal Nanocomposites Prepared via Redox Metal Translocation of Helical Polymer Metal Complexes

Manuel Núñez-Martínez, Emilio Quiñoá and Félix Freire*

Center for Research in Biological Chemistry and Molecular Materials (CiQUS)
and Department of Organic Chemistry, University of Santiago de Compostela,
E-15782 Santiago de Compostela, Spain

Electronic Supporting Information

felix.freire@usc.es

<http://felixfreire.com>

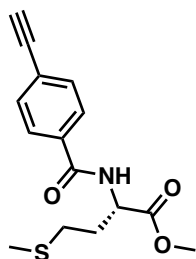
Contents

1. Molecules and Codes	4
2. Materials and methods	5
3. Synthesis of monomer M-(L)-1	6
4. Synthesis of monomer M-(L)-2	8
5. Synthesis of homopolymers	10
5.1 General procedure	10
5.2 Synthesis of polymer poly-(L)-1	10
5.3 Synthesis of polymer poly-(L)-2	11
6. Synthesis of copolymers poly-[(L)-1 _r -co-(L)-2 _{1-r}] series.....	12
7. FT-IR studies of poly-(L)-1 in presence of Ba ²⁺ ions	17
8. Stimuli responsive studies of poly-(L)-2 in presence of Au ³⁺ ions and polar and low polar solvents.....	18
9. Stimuli responsive studies of poly-[(L)-1 _r -co-(L)-2 _{1-r}] (r = 0.2-0.8) in presence of Ba ²⁺ ions.....	20
10. Preparation of poly-(L)-2-AuNPs nanocomposites	21
11. Preparation of poly-(L)-2-AgNPs nanocomposites	22
12. Preparation of poly-(L)-1-AuNPs nanocomposites	23
13. Preparation of poly-(L)-1-AgNPs nanocomposites	24
14. General procedure for the preparation of poly-[(L)-1 _r -co-(L)-2 _{1-r}]-MNPs (M = Ag or Au) nanocomposites	25
15. TEM images for poly-[(L)-1 _r -co-(L)-2 _{1-r}]-AuNPs (r = 0.8-0.2) nanocomposites.....	26
16. Influence of the amount of AuNPs in the dynamic behaviour of poly-[(L)-1 _{0.2} -co-(L)-2 _{0.8}]	26
17. Influence of the amount of AgNPs in the dynamic behaviour of poly-[(L)-1 _{0.2} -co-(L)-2 _{0.8}]	27
18. TEM images for poly-(1 _r -co-2 _{1-r})-AgNPs nanocomposites.....	28
19. TGA studies of poly-[(L)-1 _{0.2} -co-(L)-2 _{0.8}]-AuNPs and poly-[(L)-1 _{0.2} -co-(L)-2 _{0.8}]-AgNPs nanocomposites	29
20. Stability studies for poly-[(L)-1 _{0.2} -co-(L)-2 _{0.8}]-AuNPs nanocomposites	30

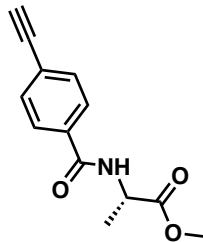
21. Stability studies for poly-[(L)-1 _{0.2} -co-(L)-2 _{0.8}]-AgNPs nanocomposites	31
22. FT-IR experiments for poly-[(L)-1 _{0.2} -co-(L)-2 _{0.8}]-MNPs (M = Au and/or Ag)	32
23. Stimuli-responsive studies: Preparation of poly-[(L)-1 _{0.2} -co-(L)-2 _{0.8}]-AgNPs in low polar and high polar solvents	33
24. Stimuli-responsive studies: Preparation of poly-[(L)-1 _{0.2} -co-(L)-2 _{0.8}]-AuNPs in low polar and high polar solvents	35
25. Control of the helical sense in poly-(1 _r -co-2 _{1-r})-AgNPs by addition of metal ions	36
26. Stimuli-responsive studies: Helical sense control of poly-[(L)-1 _{0.2} -co-(L)-2 _{0.8}]-AuNPs by addition of metal ions	38
27. SEM images for poly-[(L)-1 _{0.2} -co-(L)-2 _{0.8}]-AgNPs/Ag ⁺ nanospheres	39
28. Experiments with metal scavenger resins	40
29. Reversibility of the process with resins metal scavengers in presence of silver nanoparticles and metal ions.....	42
30. References.....	43

1. Molecules and Codes

Monomers

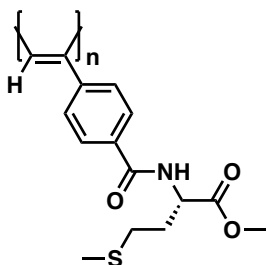


M-(L)-1

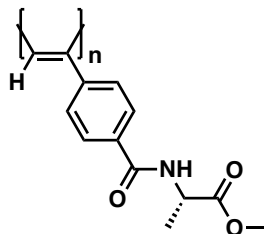


M-(L)-2

Homopolymers

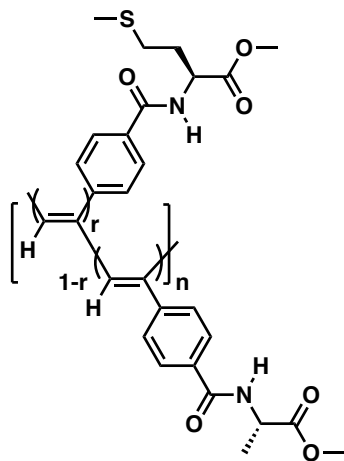


poly-(L)-1



poly-(L)-2

Copolymer



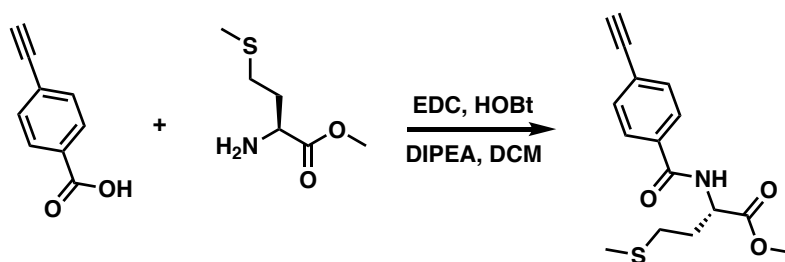
poly-[(L)-1_r-co-(L)-2_{1-r}]

2. Materials and methods

Chemicals. Commercially available chemicals have been used as delivered. Solvents were purchased as reagent grade and distilled if necessary. Anhydrous solvents were either purchased as ultra-dry solvent from Acros Organics® or received from solvent purification system. For the coupling and polymerization reactions, dry THF was obtained from MBRAUN SPS 800 solvent purification system. Water was purified by Millipore water purification system. Coupling reagents N-(3-Dimethylaminopropyl)-N'-ethylcarbodiimide hydrochloride (EDC·HCl), 1-Hydroxybenzotriazole hydrate (HOBT) and 4-ethynylbenzoic acid, were purchased from AnaSpec Inc. (L)-alanine methyl ester hydrochloride, (L)-methionine methyl ester hydrochloride, rhodium norbornadiene chloride dimer {[Rh(nbd)Cl]₂}, diisopropylethylamine (DIEA), triethylamine (TEA, 99%), sodium borohydride (NaBH₄), silver perchlorate (AgClO₄) and barium perchlorate [(Ba(ClO₄)₂], lithium perchlorate (LiClO₄) and gold(III) chloride hydrate (HAuCl₄) were purchased from Aldrich.

Instrumentations and Characterizations. NMR experiments were carried out in a Varian Inova 300 (300 MHz resonance 1H). Size exclusion chromatography studies were performed on Alliance 2695 HPLC System (Waters) liquid chromatography system equipped with a UV 2489 detector (Waters). The samples were eluted by three Phenogel columns connected to each other with stationary phases of 10³, 10⁴ and 10⁵ Amstrong and packed with a solid support of a cross-linked styrene and *p*-divinylbenzene copolymer. CD and UV measurements were registered in a Jasco-720 spectropolarimeter and a Jasco-730 spectrophotometer respectively at a nanocomposite concentration of 0.3 mg mL⁻¹. FT-IR measurements were carried out on a Bruker IFS-66v. DLS studies were performed on a Nano-ZS 90 (Malvern) equipped with a He-Ne laser (λ = 633 nm) under scattering angle of 173°. The samples were maintained at the designed temperature for 5 min before testing. DLS measurements were carried out in all cases at 0.3 mg·mL⁻¹. SEM measurements were performed on a LEO-435VP electron microscope equipped with an energy dispersive X-ray (EDX) spectrometer. TEM measurements were performed on a JEOL JEM 2010 and 200 KV as a voltage. To study the nanocomposite, or the nanospheres the same protocol was used. A dispersion of the nanocomposite or the nanospheres at a concentration of 0.3 mg mL⁻¹ was drop casted onto of silicon wafer chip and allowed to dry at rt for 12h for SEM studies, while in case of TEM studies the dispersed materials were drop-casted onto carbon chip.

3. Synthesis of monomer M-(L)-1



1-Ethyl-3-(3-dimethylaminopropyl)carbodiimide (EDC, 1.87 g, 1.2 equiv.), hydroxybenzotriazole (HOBt, 1.25 g, 1.2 equiv.), 4-ethynylbenzoic acid (1.0 g, 1.0 equiv) and diisopropyltriethylamine (DIPEA, 1.4 mL, 1.2 equiv.) were dissolved in 70 mL of CH_2Cl_2 , and the mixture was stirred for 15 min to activate the acid. Then, *L*-methionine methyl ester hydrochloride (1.92 g, 1.2 equiv) was added and the reaction mixture was stirred overnight. The organic layer was washed with HCl 1M, saturated solution of NaHCO_3 and brine. The combined organic layers were dried over anhyd Na_2SO_4 , filtered and the solvent was evaporated at reduced pressure. The crude product was chromatographed on silica gel (70-230 mesh) with hexane/ethyl acetate (7/3) as eluent [1.62 g M-(L)-1], 83% of pure product.

Spectroscopic data:

^1H NMR (300 MHz, CDCl_3) δ (ppm): 2.1 (s, 3H), 2.26 (m, 2H), 2.58 (t, 2H), 3.20 (s, 3H), 3.79 (s, 3H), 4.91 (q, 1H), 7.01 (d, 1H), 7.54 (2H, d), 7.77 (d, 2H).

^{13}C NMR (75 MHz, CDCl_3) δ (ppm): 15.7, 30.2, 31.6, 52.3, 52.8, 79.8, 82.8, 125.9, 127.2, 132.4, 133.8, 166.4, 172.6.

$[\alpha]_D^{20} = +42$ (10 mg mL^{-1} , CHCl_3)

HRM (ESI) m/z calcd for $\text{C}_{15}\text{H}_{17}\text{NO}_3\text{S}$ $[\text{M}+\text{Na}]^+$: 314.0821, found: 314.0823.

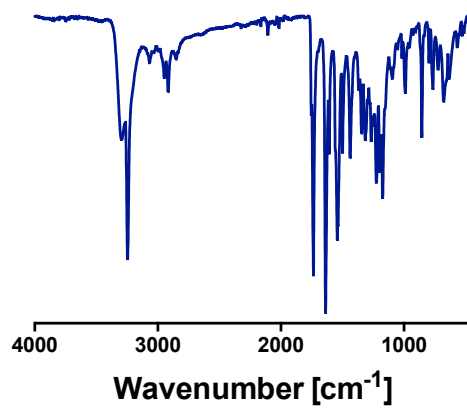


Figure S1. FT-IR spectrum of M-(L)-1.

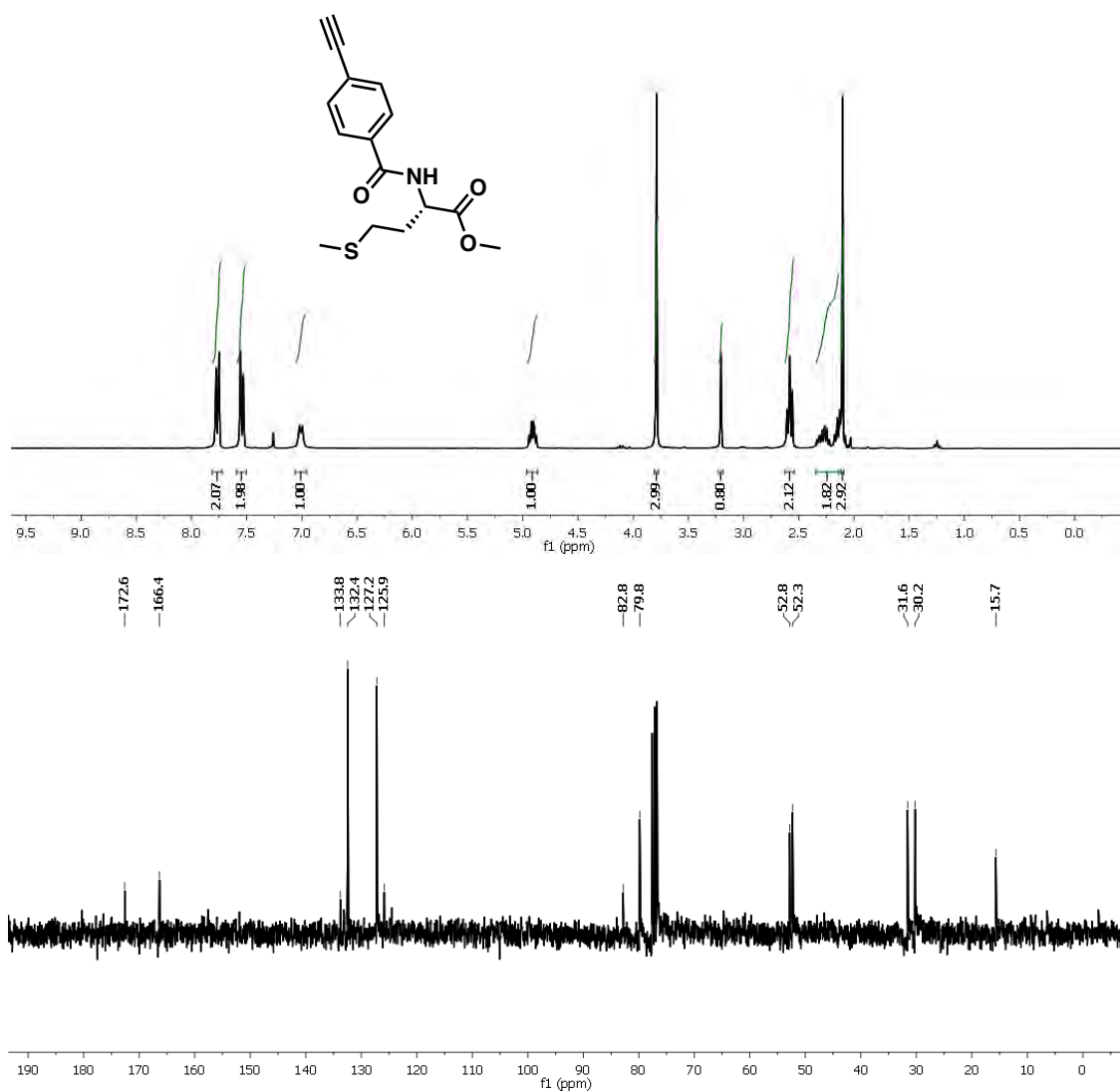
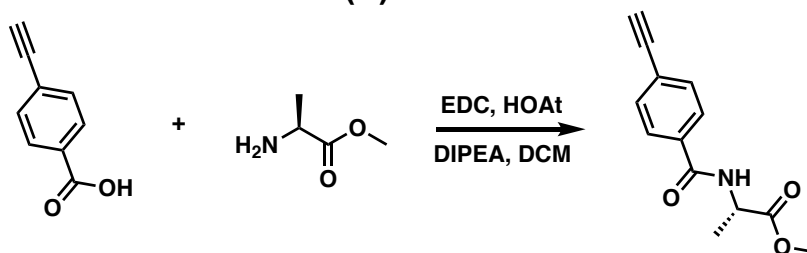


Figure S2. ¹H NMR and ¹³C NMR spectra of M-(L)-1 in CDCl₃.

4. Synthesis of monomer M-(L)-2



1-Ethyl-3-(3-dimethylaminopropyl)carbodiimide (EDC, 0.656 g, 1.2 equiv), hydroxybenzotriazole (HOBt, 0.465 g, 1.2 equiv), 4-ethynylbenzoic acid (0.500 g, 1.2 equiv) and diisopropyltriethylamine (DIPEA, 0.596 mL, 1.2 equiv) were dissolved in 70 mL of CH₂Cl₂, and the mixture was stirred for 15 min to activate the acid. Then, methyl L-Alaninate (0.388 g, 1.0 equiv) was added and the reaction mixture was stirred overnight. The organic layer was washed with HCl 1M, saturated solution of NaHCO₃ and brine. The combined organic layers were dried over anhyd Na₂SO₄, filtered and the solvent was evaporated at reduced pressure. The crude product was chromatographed on silica gel (70-230 mesh) with hexane/ethyl acetate (7/3) as eluent [0.503 g M-(L)-2], 76% of pure product.

Spectroscopic data:

¹H NMR (300 MHz, CDCl₃) δ (ppm): 1.49 (d, 3H), 3.25 (s, 1H), 3.74 (s, 3H), 4.75 (q, 1H), 7.29 (d, 1H), 7.48 (d, 2H), 7.76 (d, 2H).

¹³C NMR (75 MHz, CDCl₃) δ (ppm): 18.0, 48.5, 52.4, 79.7, 82.7, 125.4, 127.1, 132.0, 133.6, 166.2, 173.5.

[α]_D²⁰ = +81 (15 mg mL⁻¹, CHCl₃).

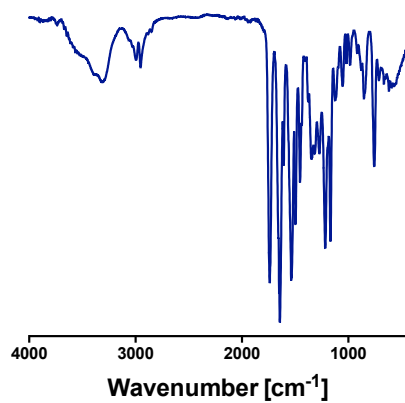


Figure S3. FT-IR spectrum for M-(L)-2.

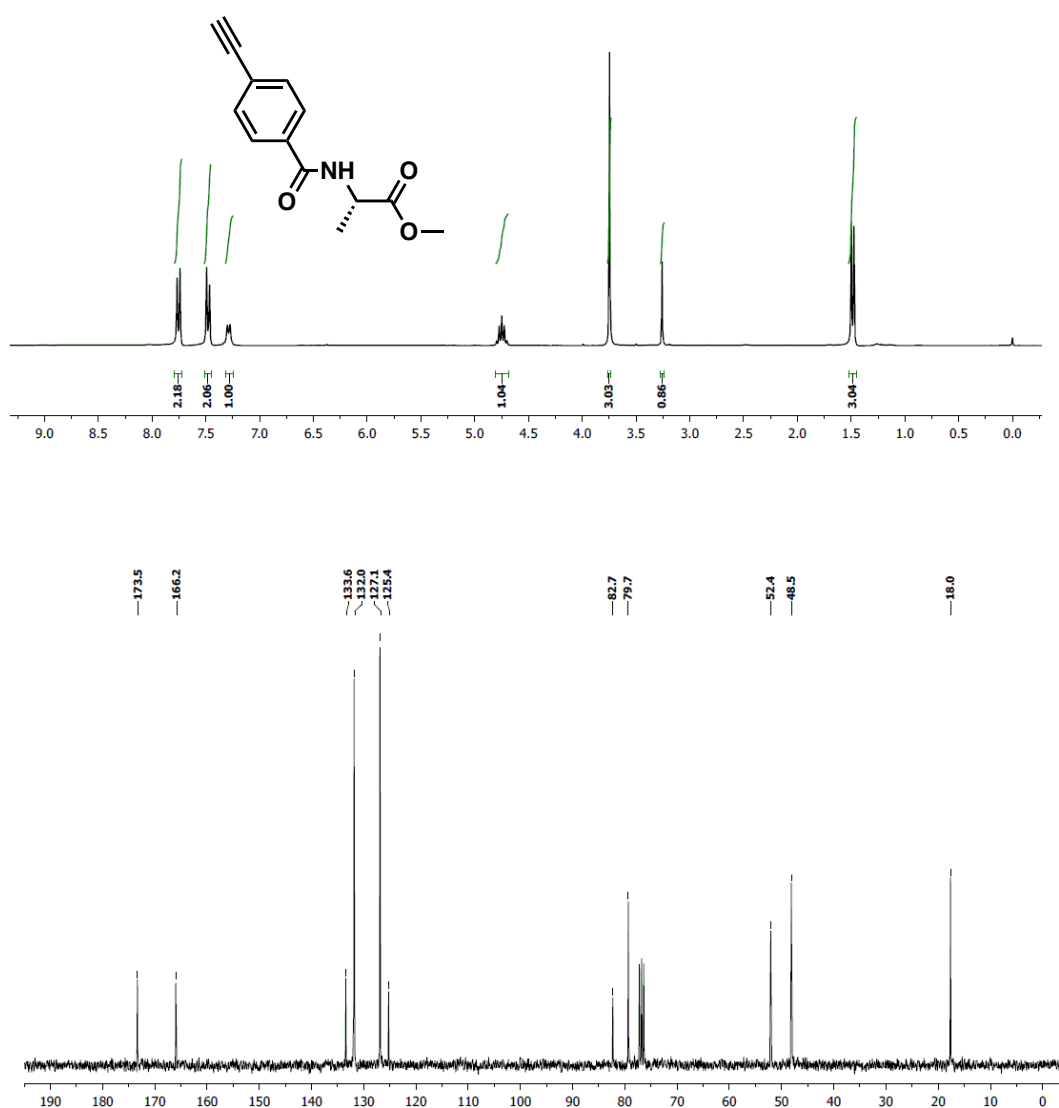


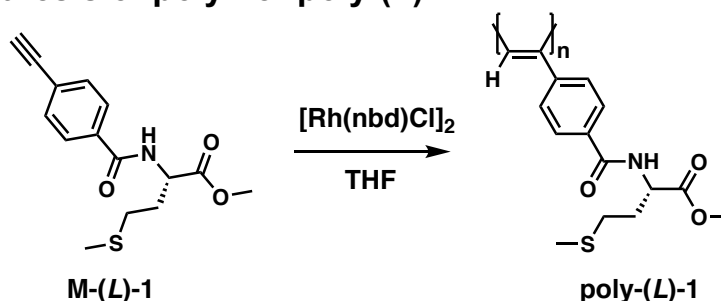
Figure S4. ¹H and ¹³C NMR of monomer M-(L)-2 in CDCl₃.

5. Synthesis of homopolymers

5.1 General procedure

The polymer was synthesized in a reaction flask (sealed ampoule) that was dried under vacuum and flushed with argon for three times before monomers were added as a solid. Then, the flask was evacuated on a vacuum line and flushed with dry argon (three times). Dry THF was added with a syringe and then, Et₃N dropwise. A solution of rhodium norbornadiene chloride dimer, [Rh(nbd)Cl]₂, in THF was added at 30 °C. The reaction mixture was stirred at 60 °C for 1 h. Next, the resulting polymer was diluted in CH₂Cl₂ and they were precipitated in a large amount of diethyl ether, centrifuged (twice) and re-precipitated in hexane and centrifuged again.

5.2 Synthesis of polymer poly-(L)-1



Following the general procedure, **M-(L)-1** (60 mg, 0.206 mmol), Et₃N (5 μL) and [Rh(nbd)Cl]₂ (0.94 mg) in THF (0.412 mL) yielded after centrifugation (88%) of **poly-(L)-1**.

GPC data: $M_n = 13585$, $M_w = 33002$, $M_p = 12283$, $M_z = 93739$, PDI = 2.42.

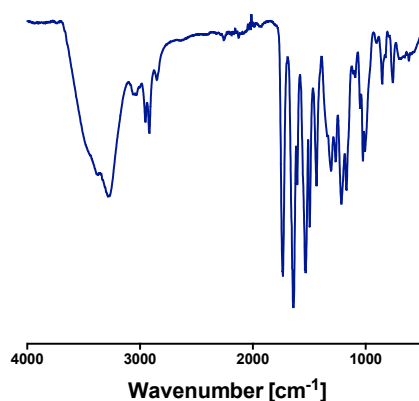


Figure S5. FT-IR spectrum of **poly-(L)-1**.

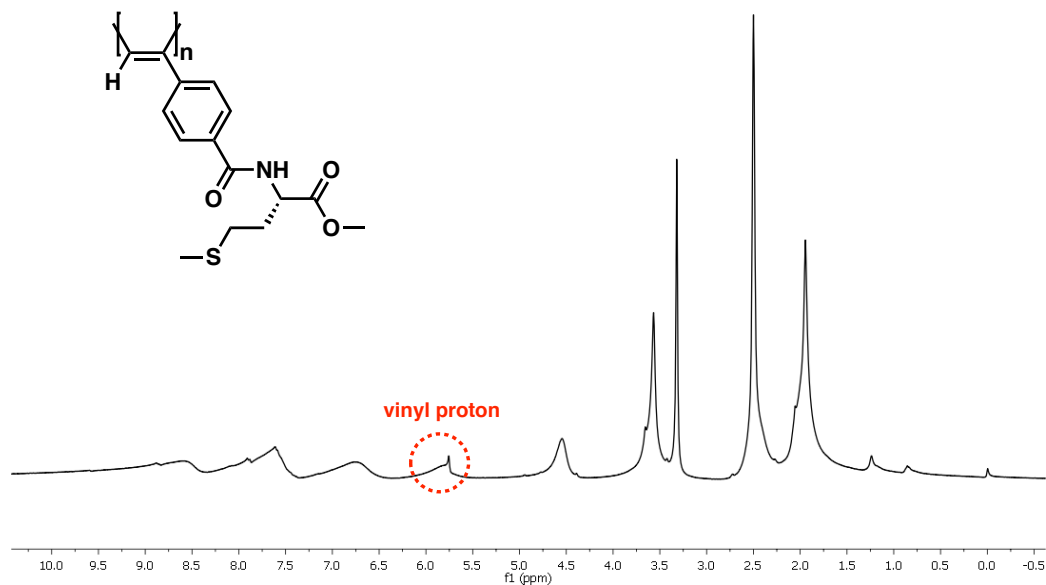
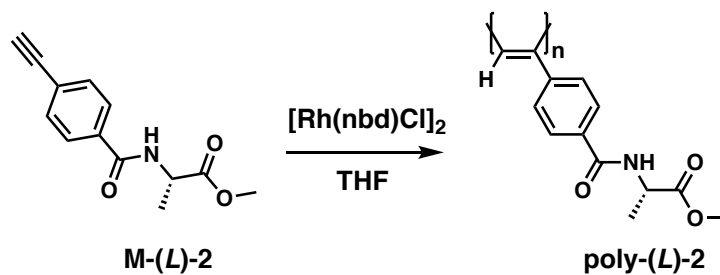


Figure S6. ^1H NMR spectrum of poly-(L)-1 in DMSO-d_6 .

5.3 Synthesis of polymer poly-(L)-2



Following the general procedure, M-(L)-2 (100 mg, 0.433 mmol), Et_3N (5 μL) and $[\text{Rh}(\text{nbd})\text{Cl}]_2$ (1.98 mg) in THF (0.860 mL) yielded after centrifugation (91%) of poly-(L)-2.

GPC data: $M_n = 8989$, $M_w = 35877$, $M_p = 8374$, $M_z = 250055$, $\text{PDI} = 3.99$.

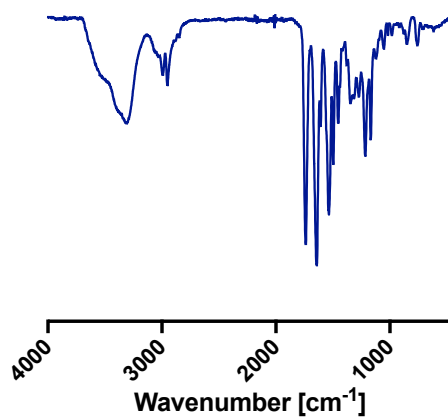


Figure S7. FT-IR spectrum of poly-(L)-2.

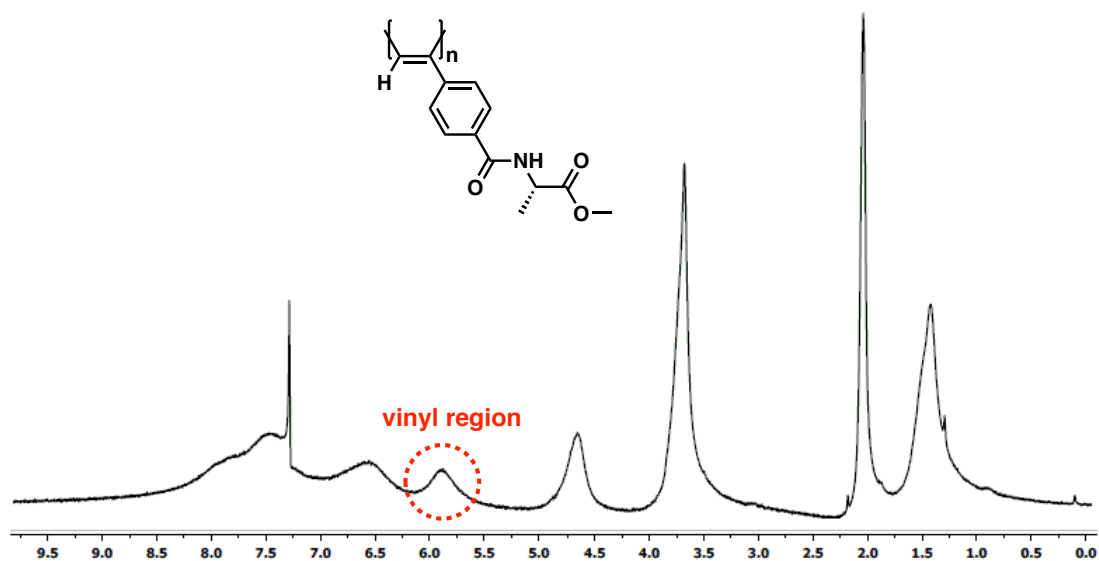
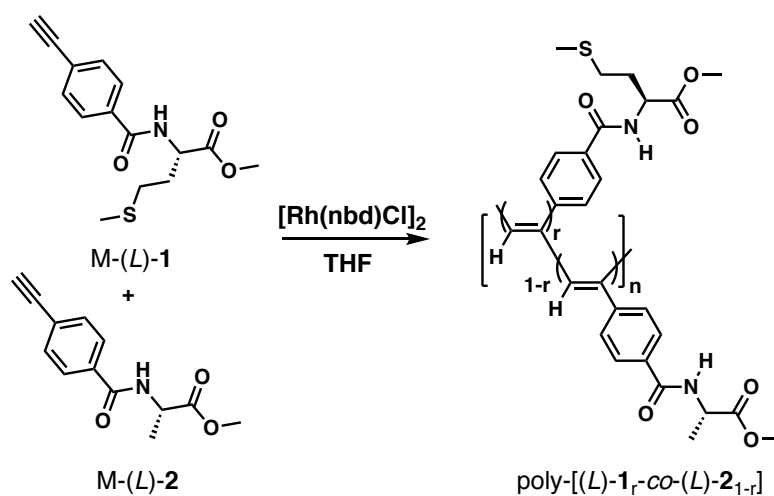


Figure S8. ^1H NMR spectrum of poly-(L)-2 in CDCl_3 .

6. Synthesis of copolymers poly-[(L)-1_r-co-(L)-2_{1-r}] series



Following the general procedure, poly-[(L)-1_r-co-(L)-2_{1-r}] series was synthesized according to the different amounts of reagents M-(L)-1 and M-(L)-2, Et_3N , $[\text{Rh}(\text{nbd})\text{Cl}]_2$ and THF) reported in the table S1. The *cis* stereoregularity of the copolymers was determined by ^1H NMR where the vinyl proton resonance is between 5.6-5.9 ppm.

Table S1. Quantities of monomers, Et₃N, [Rh(nbd)Cl]₂ and THF.

Copolymer	M1	M2	Et ₃ N	[Rh(nbd)Cl] ₂	THF	Yield
			(μ L)	(mg)	(mL)	(%)
Poly-[(L)-1 _{0.8} -co-(L)-2 _{0.2}]	83	17	5	2	0.87	85
Poly-[(L)-1 _{0.6} -co-(L)-2 _{0.4}]	65	35	5	2	0.87	81
Poly-[(L)-1 _{0.4} -co-(L)-2 _{0.6}]	45	55	5	2	0.87	91
Poly-[(L)-1 _{0.2} -co-(L)-2 _{0.8}]	24	76	5	2	0.87	80

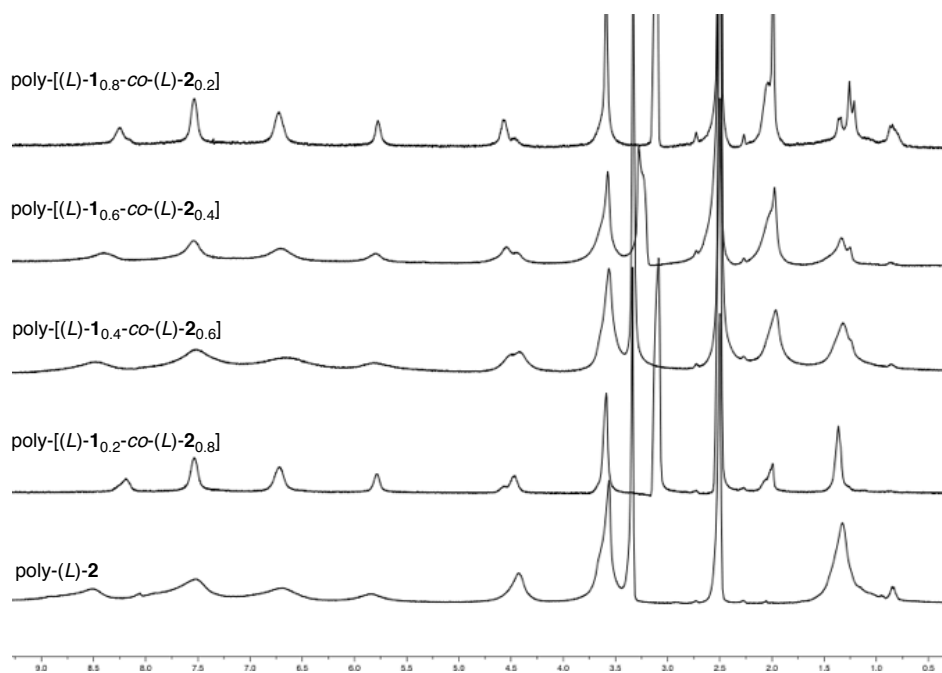


Figure S9. ¹H NMR of poly-[(L)-1_r-co-(L)-2_{1-r}] ($r = 0.8-0.2$) and poly-(L)-2 series of copolymers (DMSO-d₆, 300 MHz).

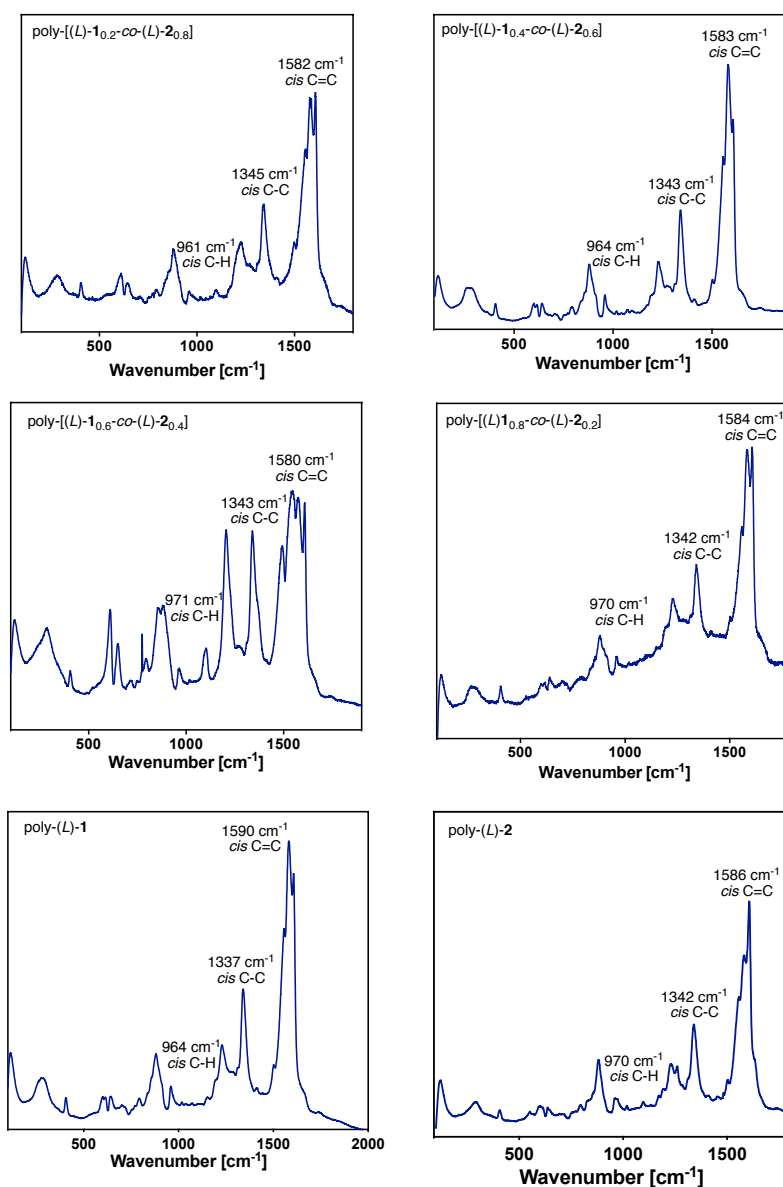


Figure S10. Raman spectra for copolymers poly-[(L)-1-co-(L)-2]_{1-r} (r = 0.8-0.2) series.

DSC studies were carried out to determine the geometry of the polymer backbone. As a general protocol, a polymer sample was kept in an aluminium pan and heated from 40 °C to 350 °C with a heating rate of 10 °C min⁻¹.

- DSC studies of poly-[(L)-1_r-co-(L)-2_{1-r}] (r = 0.8-0.2)

The thermograms of the polymers showed typical traces for a *cis-trans* backbone, where two exothermal peaks corresponding to the *c-t* to *c-c* and the *c-c* to *t-t* were observed.

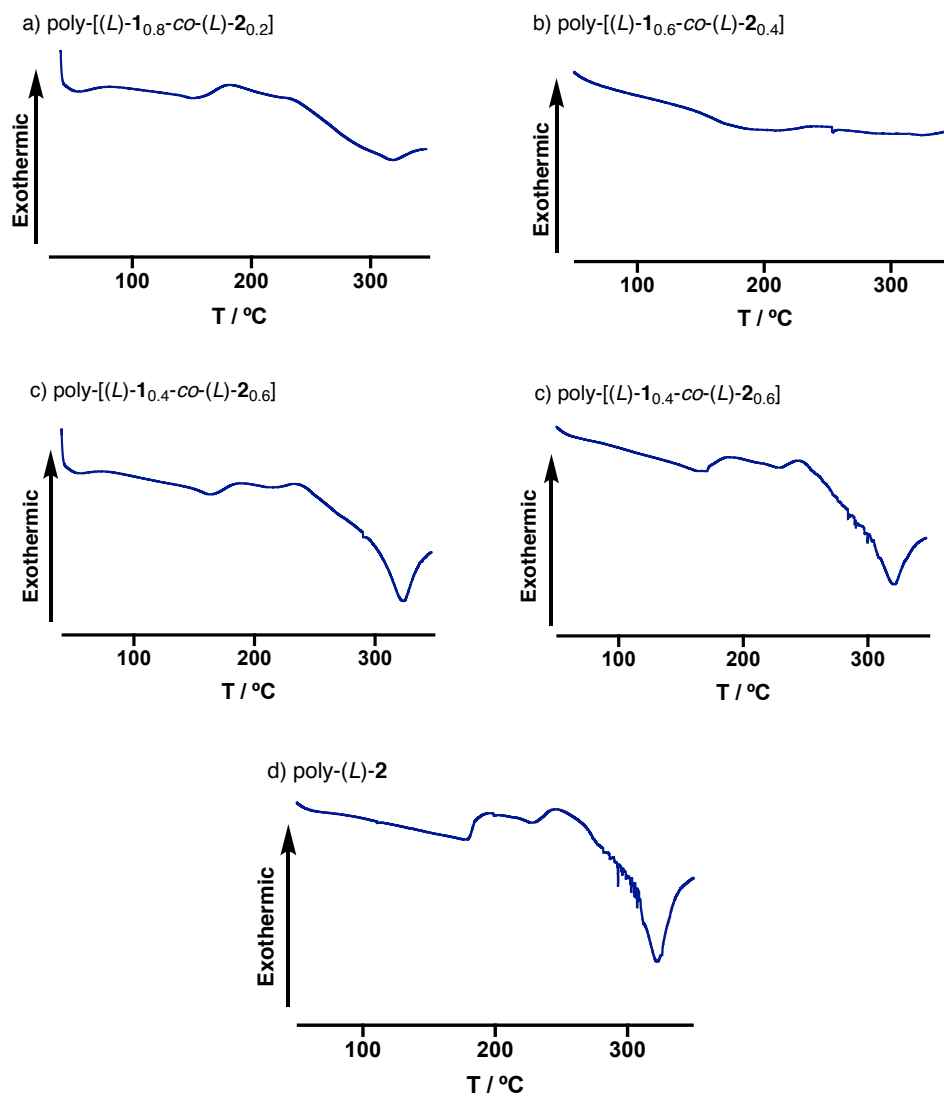


Figure S11. DSC studies of poly-[(L)-1_r-co-(L)-2_{1-r}] (r = 0.8-0.2) series of copolymers.

- TGA studies of poly-[(L)-1_r-co-(L)-2_{1-r}] (r = 0.8-0.2) series

TGA Studies were carried out to determine the thermal stability of the copolymers. As a general protocol, a copolymer sample was kept in a platinum pan and heated from 40 °C to 850 °C with a heating rate of 10 °C min⁻¹.

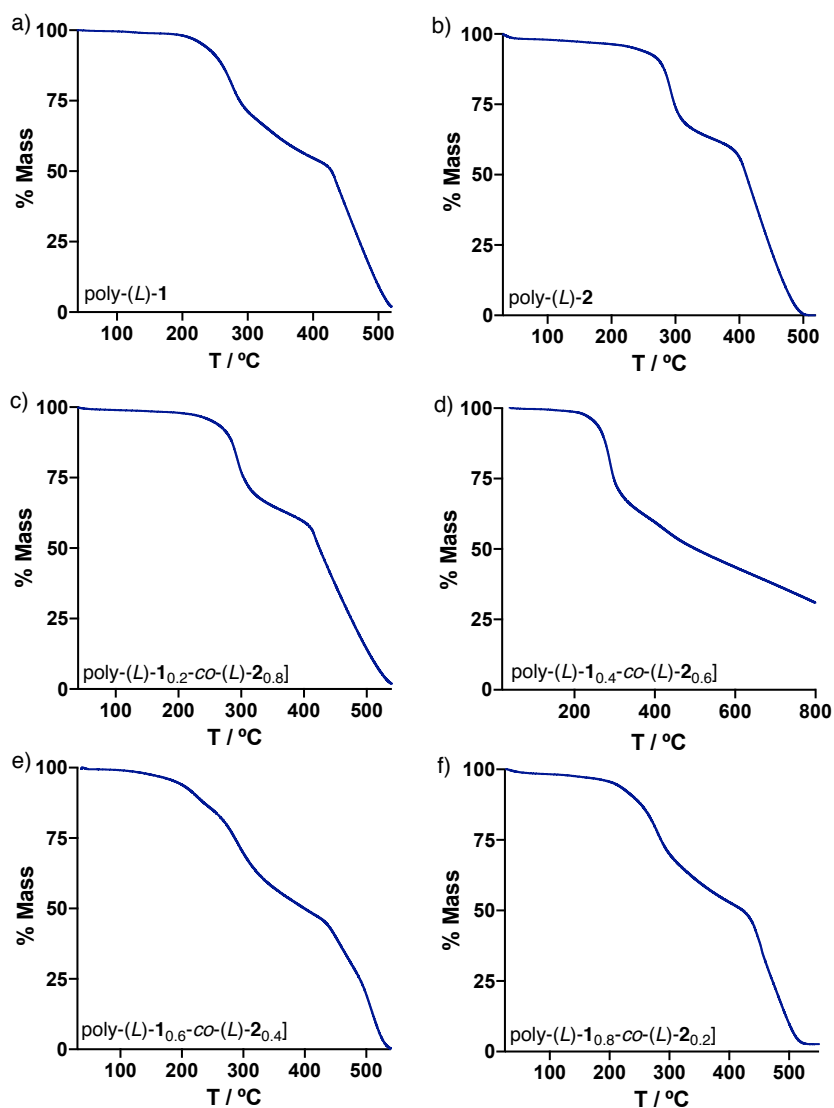
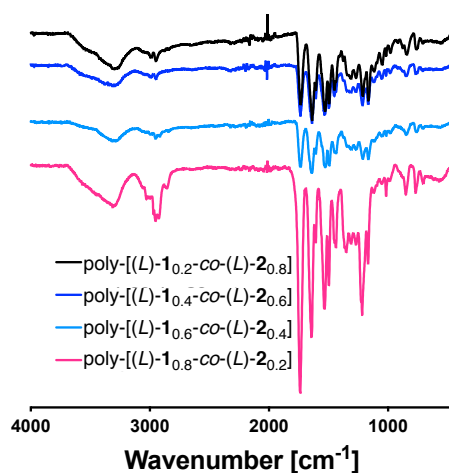


Figure S12. TGA studies of poly-[(L)-1_r-co-(L)-2_{1-r}] (r = 0.8-0.2) series of copolymers.

Table S2. GPC data of the copolymers.

Polymer	M_n	M_w	M_p	M_z	PDI
Poly-(L)-2	8989	35877	8374	250055	3.99
Poly-[(L)-1 _{0.8} -co-(L)-2 _{0.2}]	5281	23296	7395	129509	4.41
Poly-[(L)-1 _{0.6} -co-(L)-2 _{0.4}]	5186	19214	7939	78399	3.70
Poly-[(L)-1 _{0.4} -co-(L)-2 _{0.6}]	8780	40844	20269	157407	4.65
Poly-[(L)-1 _{0.2} -co-(L)-2 _{0.8}]	7690	9226	7759	11161	1.20

**Figure S13.** FT-IR spectra of poly-[(L)-1_r-co-(L)-2_{1-r}] ($r = 0.8-0.2$) series of copolymers.

7. FT-IR studies of poly-(L)-1 in presence of Ba²⁺ ions

ATR/FT-IR spectra were recorded in a BRUKER IFS-66v spectrophotometer. A solution of Ba(ClO₄)₂ (0.5 equiv, 10.0 mg mL⁻¹ in MeOH) was added to a solution of poly-(L)-1 in CHCl₃ (0.3 mg mL⁻¹) and then the FT-IR spectrum were registered. The experiments confirmed the coordination of Ba²⁺ to both carbonyl groups in poly-(L)-1.

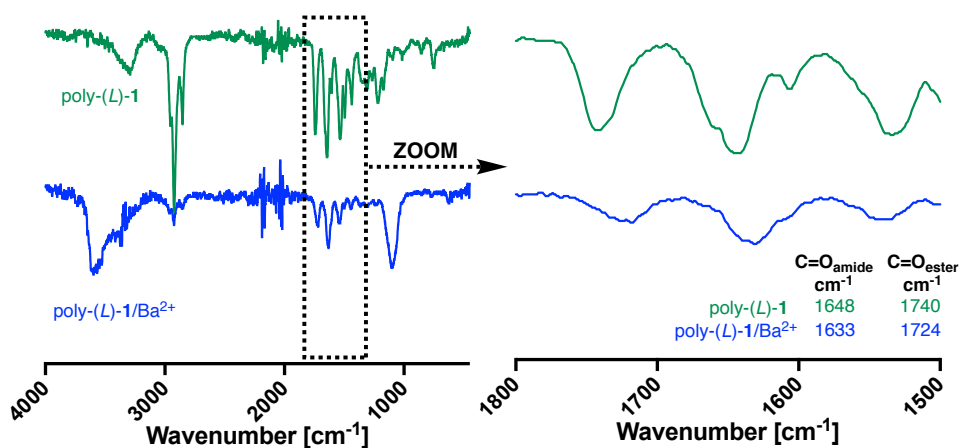


Figure S14. FT-IR spectra of poly-(L)-1 and poly-(L)-1/Ba²⁺ complexes.

8. Stimuli responsive studies of poly-(L)-2 in presence of Au³⁺ ions and polar and low polar solvents

Stimuli-responsive studies in presence of Au³⁺ ions and polar and low polar solvents were carried out to determine the dynamic properties of poly-(L)-2.

For that, CD studies were carried out with a solution of poly-(L)-2 (0.3 mg mL⁻¹) in CHCl₃ in presence of HAuCl₄ (10 mg mL⁻¹ in MeOH) as source of Au³⁺ ions.

Thus, poly-(L)-2 dissolved in CHCl₃ showed the formation of *M* helices (CD₃₇₀ < 0) corresponding to an *anti* conformation between carbonyl groups. On the other hand, the addition of 0.4 equiv of Au³⁺ ions to poly-(L)-2 promoted an helical inversion (*P* helices, CD₃₇₀ > 0) due to the coordination of the Au³⁺ ions to the carbonyl groups in an *anti* conformation.

Moreover, the solution of poly-(L)-2 in low polar solvents (CHCl₃, DCM) lead to the formation of *M* helices (CD₃₇₀ < 0, *anti* conformation) whereas the solution of poly-(L)-2 in high polar solvents (DMF, DMSO) formed the opposite helical sense (*P* helices, CD₃₇₀ > 0).

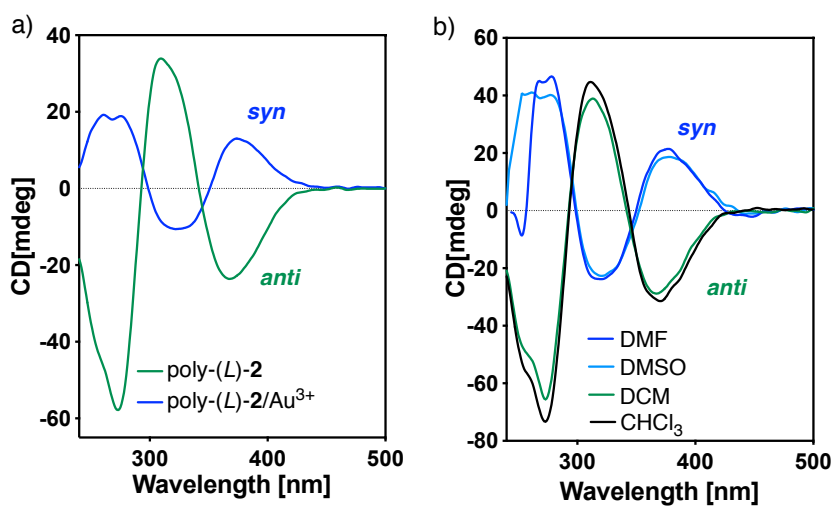
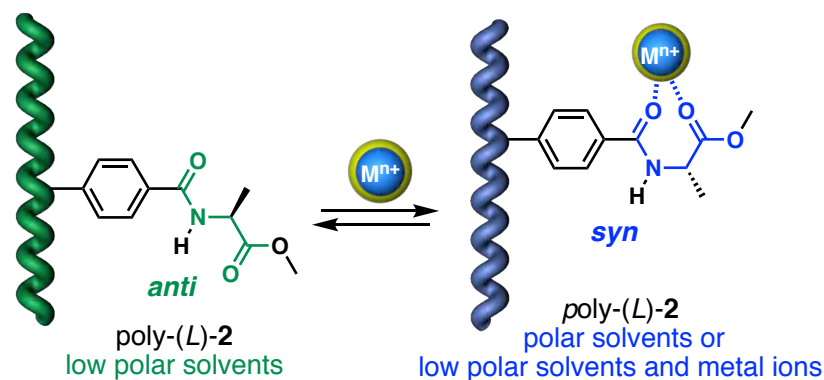


Figure S15. CD studies for the preparation of poly-(L)-2 in presence of Au³⁺ ions and low poly and high polar solvents.

The coordination of Au³⁺ ions to poly-(L)-2 was checked by FT-IR experiments. A solution of HAuCl₄ (0.5 equiv, 10.0 mg mL⁻¹ in MeOH) was added to a solution of poly-(L)-2 in CHCl₃ (0.3 mg mL⁻¹) and then the FT-IR spectrum were registered. The experiments confirmed the coordination of Au³⁺ to both carbonyl groups in poly-(L)-2.

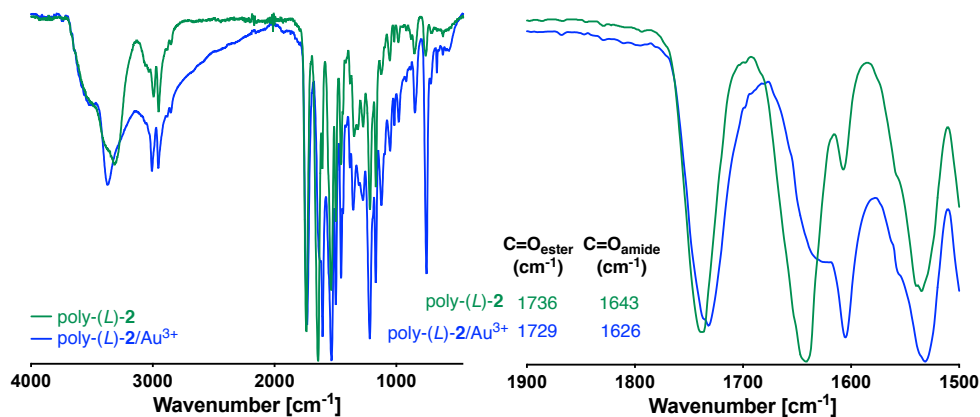
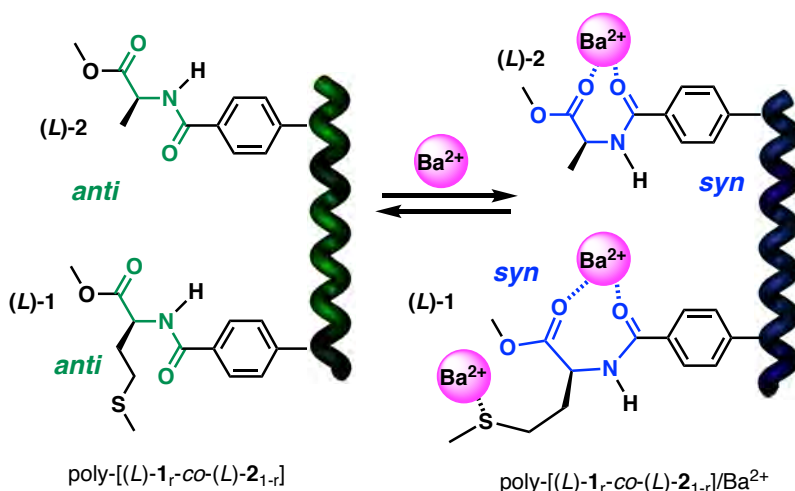


Figure S16. FT-IR spectra of poly-(L)-2 and poly-(L)-2/Au³⁺ complexes.

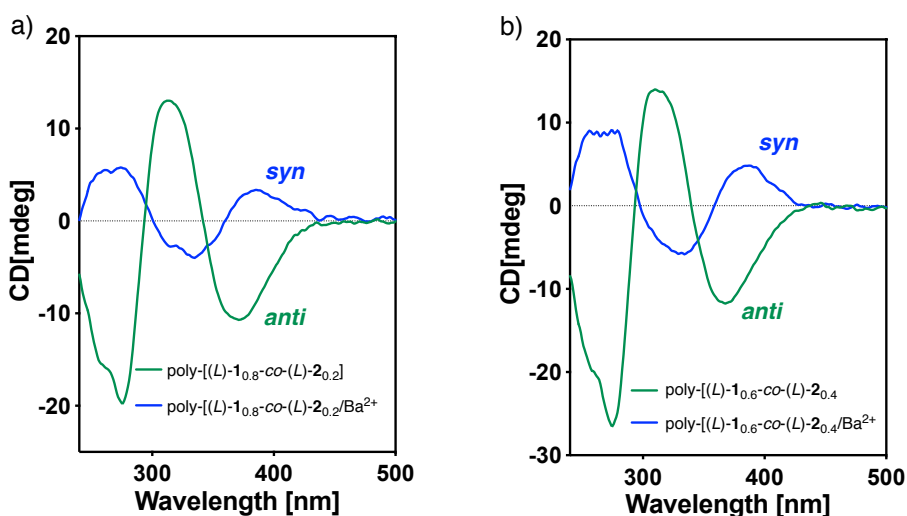
9. Stimuli responsive studies of poly-[(L)-1_r-co-(L)-2_{1-r}] (r = 0.2-0.8) in presence of Ba²⁺ ions



Stimuli-responsive studies of poly-[(L)-1_r-co-(L)-2_{1-r}] (r = 0.8-0.2) in presence of Ba²⁺ ions were carried out to determine the dynamic properties of the PPAs.

For that, CD studies were carried out with a solution of poly-[(L)-1_r-co-(L)-2_{1-r}] (r = 0.2-0.8) (0.3 mg mL⁻¹) in CHCl₃ in presence of BaClO₄ (10 mg mL⁻¹ in MeOH) as source of Ba²⁺ ions.

Thus, poly-[(L)-1_r-co-(L)-2_{1-r}] (r = 0.2-0.8) in CHCl₃ showed the formation of *M* helices (CD₃₇₀ < 0) corresponding to an *anti* conformation between carbonyl groups. On the other hand, the addition 0.4 equiv of Ba²⁺ ions to poly-[(L)-1_r-co-(L)-2_{1-r}] (r = 0.2-0.8) promoted an helical inversion (*P* helices, CD₃₇₀ > 0) due to the coordination of the Ba²⁺ ions to the carbonyl groups in a *syn* conformation.



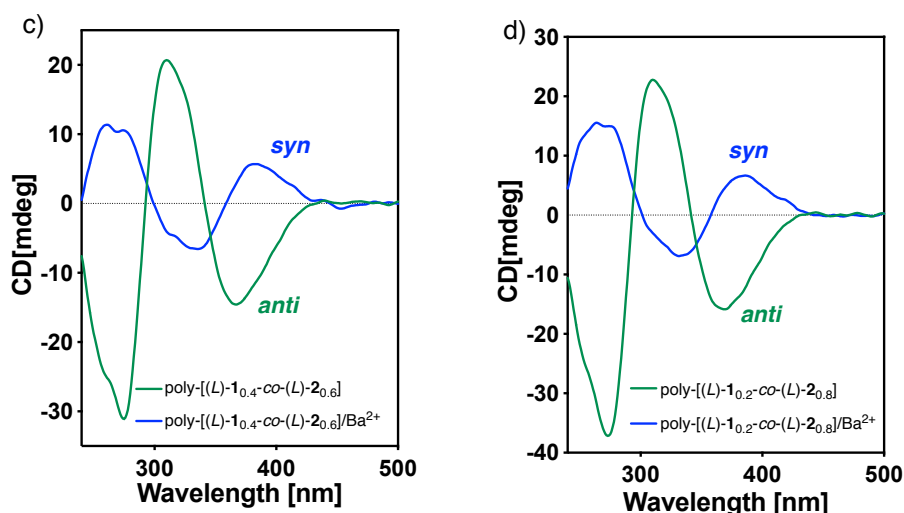


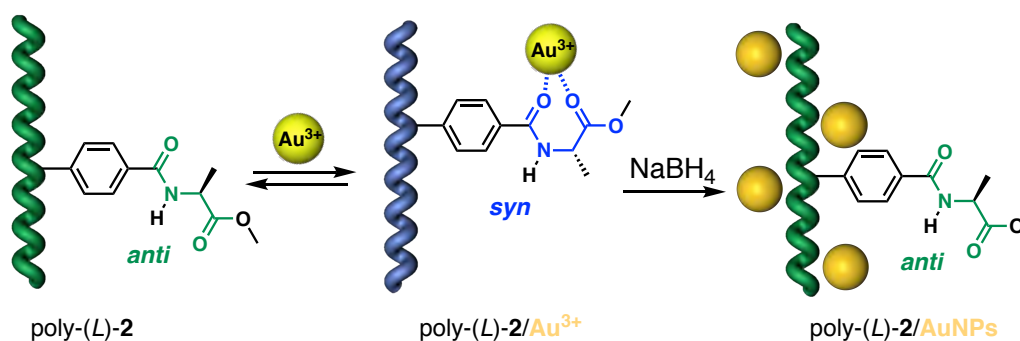
Figure S17. a) CD and UV studies of poly-[(L)-1_{0.8}-co-(L)-2_{0.2}] in presence of Ba²⁺ ions. b) CD and UV studies of poly-[(L)-1_{0.6}-co-(L)-2_{0.4}] in presence of Ba²⁺ ions. c) CD and UV studies of poly-[(L)-1_{0.4}-co-(L)-2_{0.6}] in presence of Ba²⁺ ions. d) CD and UV studies of poly-[(L)-1_{0.2}-co-(L)-2_{0.8}] in presence of Ba²⁺ ions.

10. Preparation of poly-(L)-2-AuNPs nanocomposites

A solution of poly-(L)-2 (0.3 mg mL⁻¹) in CHCl₃ (CD₃₇₀ < 0, *M* helices) is titrated with 0.5 equiv of HAuCl₄ (10 mg mL⁻¹, MeOH) to form a poly-(L)-2/Au³⁺ complexes resulting an helical inversion (CD₃₇₀ > 0, *P* helices). Finally, the addition of 1.0 equiv of NaBH₄ (1 mg mL⁻¹, MeOH) form poly-(L)-2-AuNPs.

UV-Vis showed the presence of a classical small localized plasmon surface resonance (LSPR) band nm corresponding to the formation of spherical AuNPs.

TEM images confirm the formation of high polydisperse spherical AuNPs. Furthermore, the AuNPs have shown a poor stability in solution.



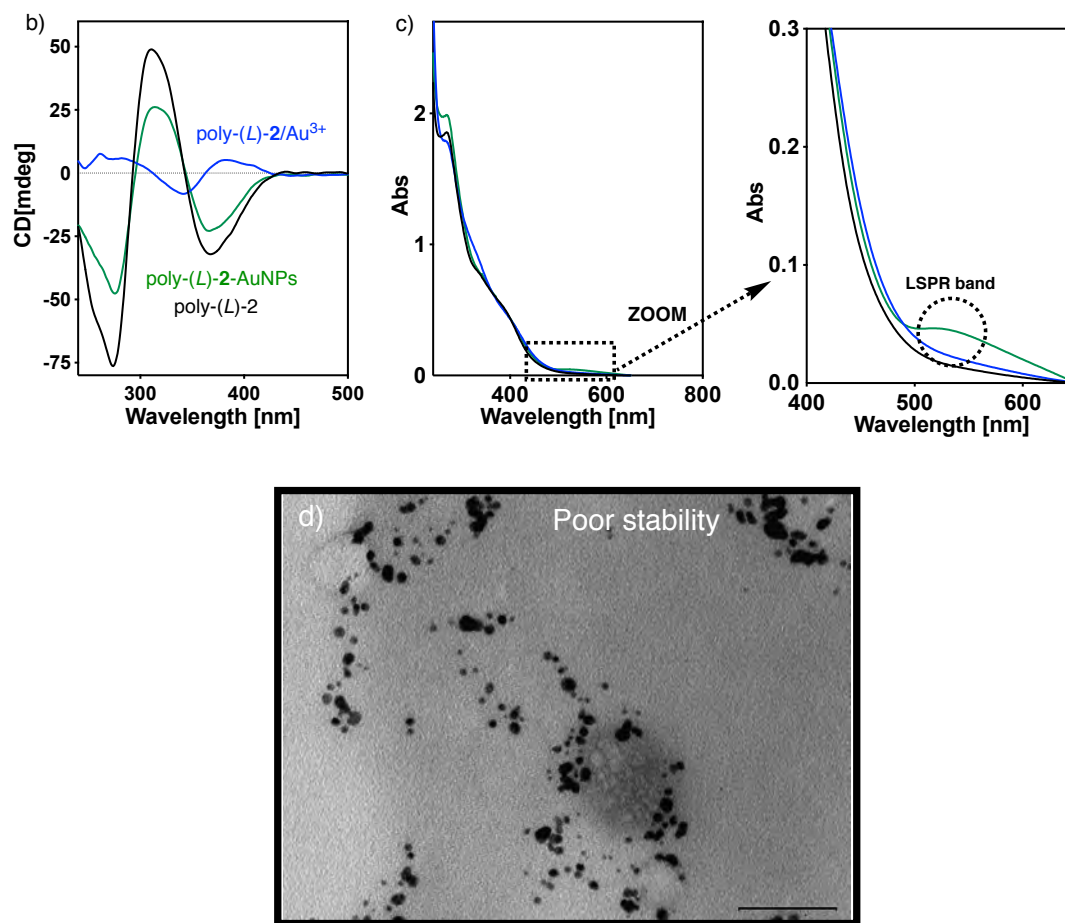


Figure S18. a) Schematic representation for the preparation for poly-(L)-2-AuNPs nanocomposites. b) CD traces for poly-(L)-2, poly-(L)-2/Au³⁺ complexes and poly-(L)-2-AuNPs nanocomposites. c) UV-Vis experiments for poly-(L)-2, poly-(L)-2/Au³⁺ complexes and poly-(L)-2-AuNPs nanocomposites. d) TEM image for poly-(L)-2-AuNPs nanocomposites.

11. Preparation of poly-(L)-2-AgNPs nanocomposites

A solution of poly-(L)-2 (0.3 mg mL⁻¹) in CHCl₃ (CD₃₇₀ < 0, *M* helices) is titrated with 0.5 equiv. of AgClO₄ (10 mg mL⁻¹, MeOH) to form a poly-(L)-2/Ag⁺ complexes resulting an helical inversion (CD₃₇₀ > 0, *P* helices). Finally, the addition of 1.0 equiv. of NaBH₄ (1 mg mL⁻¹, MeOH) form poly-(L)-2-AgNPs.

UV-Vis showed the presence of the typical localized plasmon surface resonance (LSPR) band corresponding to the formation of spherical AgNPs. UV-Vis spectrum after 24 hours showed a strong depletion in the LSPR band indicating a poor stability of the AgNPs.

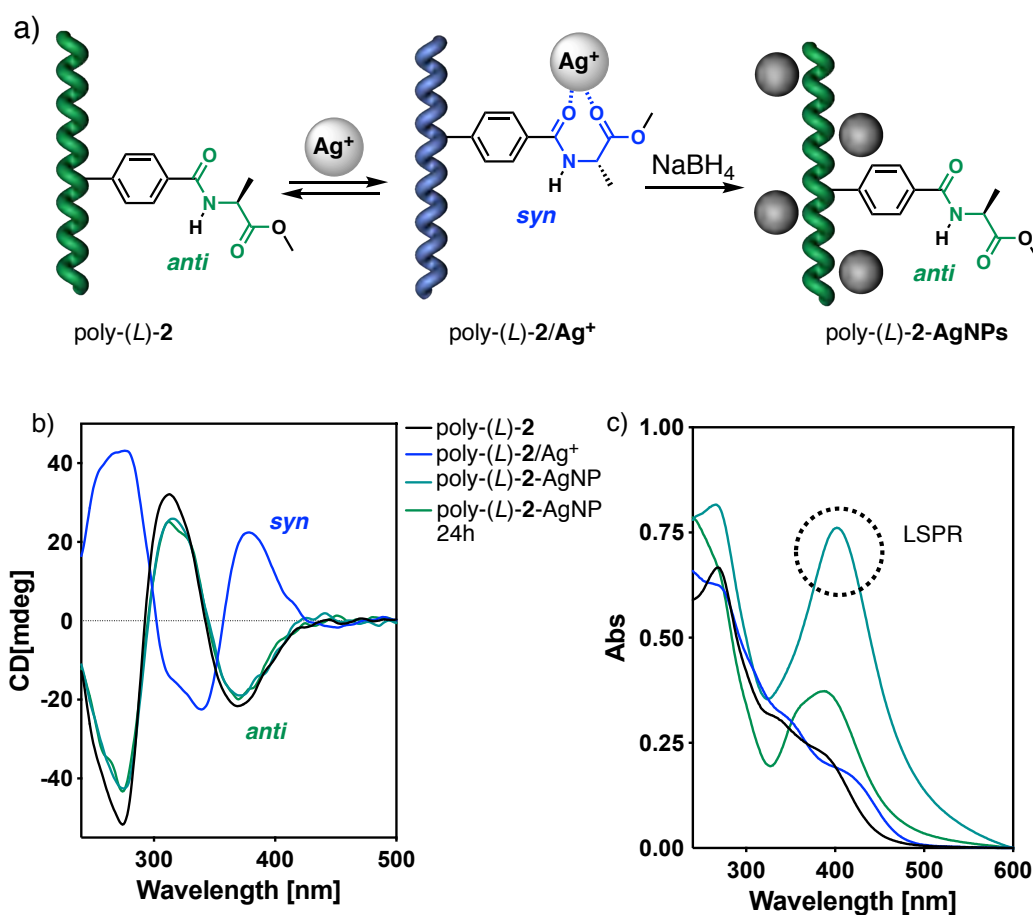
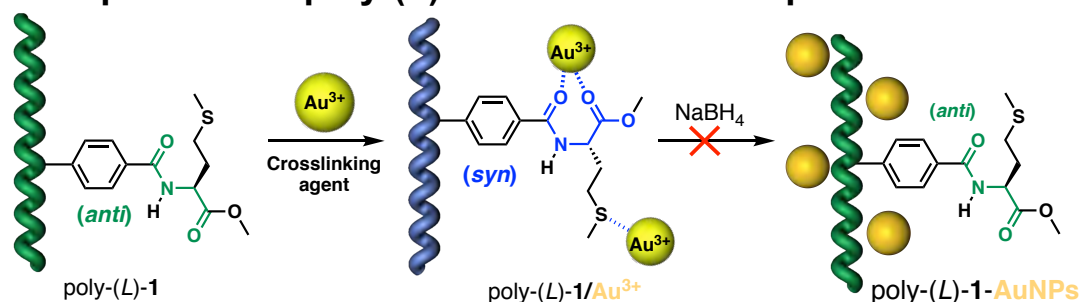


Figure S19. a) Schematic representation for the preparation for poly(L)-2-AgNPs nanocomposites. b) CD traces for poly(L)-2, poly(L)-2/Ag⁺ complexes, poly(L)-2-AgNPs nanocomposites and poly(L)-2-AgNPs at 24 hours. c) UV-Vis experiments CD traces for poly(L)-2, poly(L)-2/Ag⁺ complexes, poly(L)-2-AgNPs nanocomposites and poly(L)-2-AgNPs at 24 hours.

12. Preparation of poly(L)-1-AuNPs nanocomposites



The general protocol to form the nanocomposites was employed to determine the ability of poly(L)-1 as stabilizing agent of AuNPs.

For that, CD studies of poly(L)-1 in CHCl_3 (0.3 mg mL^{-1}) showed the formation of *M* helices ($\text{CD}_{370} < 0$) corresponding an *anti* conformation between carbonyl groups.

Interestingly, the addition of 0.5 equiv HAuCl_4 (10 mg mL^{-1} , MeOH) to poly-(L)-1 showed the aggregation of the polymer chains leading to null CD in the vinylic region (370 nm). The aggregation of PPAs chains avoided the ulterior formation of the AuNPs.

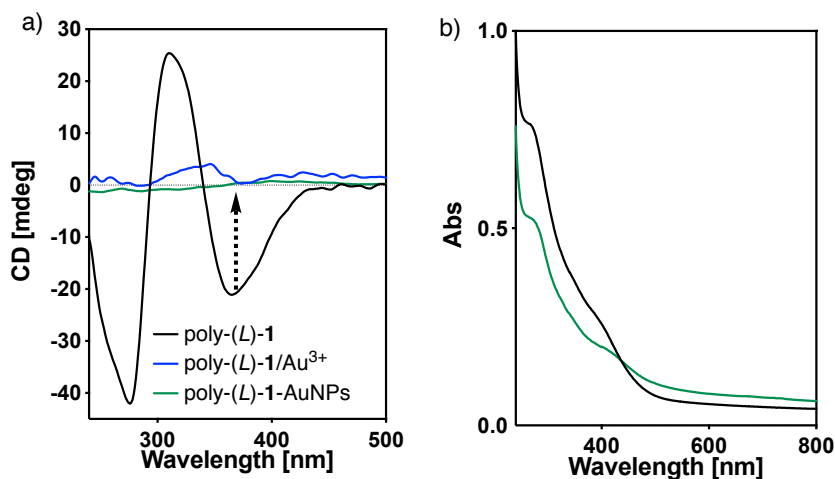
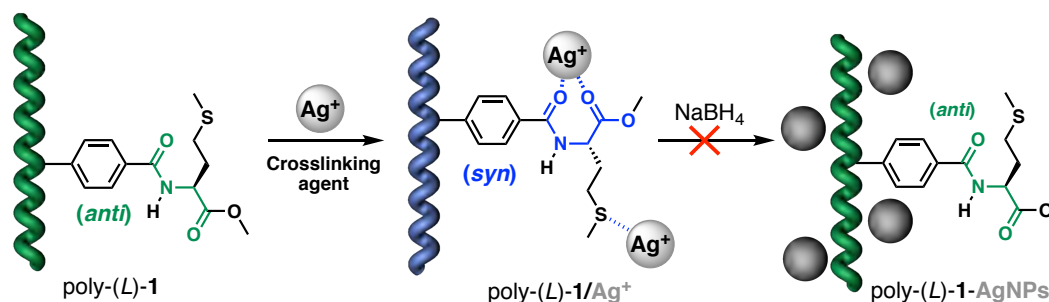


Figure S20. a) CD and b) UV studies for the preparation of poly-(L)-1-AuNPs nanocomposites.

13. Preparation of poly-(L)-1-AgNPs nanocomposites



The general protocol to form the nanocomposites was employed to determine the ability of poly-(L)-1 as stabilizing agent of AgNPs.

For that, CD studies of poly-(L)-1 in CHCl_3 (0.3 mg mL^{-1}) showed the formation of *M* helices ($\text{CD}_{370} < 0$) corresponding an *anti* conformation between carbonyl groups. Interestingly, the addition of 0.5 equiv AgClO_4 (10 mg mL^{-1} , MeOH) to poly-(L)-1 showed the aggregation of the polymer chains leading to null CD in the vinylic region (370 nm). The aggregation of PPAs chaing avoided the ulterior formation of the AgNPs.

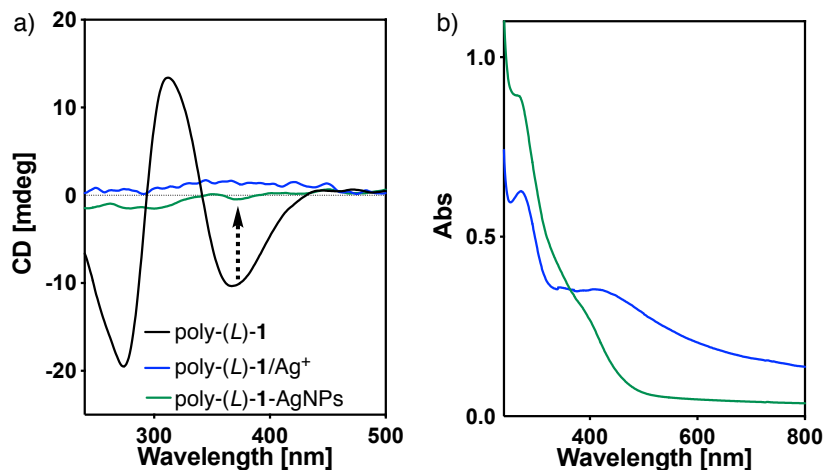


Figure S21. a) CD and b) UV studies for the preparation poly-(L)-1-AgNPs nanocomposites.

14. General procedure for the preparation of poly-[(L)-1_r-co-(L)-2_{1-r}]-MNPs (M = Ag or Au) nanocomposites

Poly-[(L)-1_{0.2}-co-(L)-2_{0.8}]-MNPs (M = Au, Ag) nanocomposites were prepared according to this procedure. First, all the glassware was washed with aqua regia, Milli Q water and acetone. The reaction was carried out at room temperature and using Ar atmosphere.

Poly-[(L)-1_{0.2}-co-(L)-2_{0.8}] was dissolved in CHCl₃ (0.3 mg mL⁻¹) and then, HAuCl₄ (10 mg mL⁻¹) as source of Au³⁺ ions or AgClO₄ (0.5 equiv.) as source of Ag⁺ ions in MeOH were added to form the poly-(1_r-co-2_{1-r})/Mⁿ⁺ (Mⁿ⁺ = Au³⁺, Ag⁺) complexes. Next, NaBH₄ (1.0 equiv., 1.0 mg mL⁻¹) in MeOH was added to form Poly-[(L)-1_{0.2}-co-(L)-2_{0.8}]-MNPs (M = Ag or Au) nanocomposites.

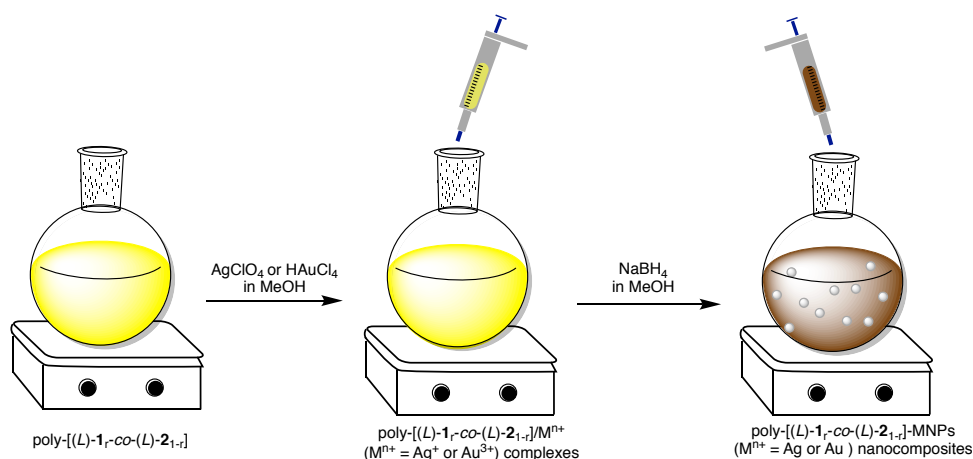


Figure S22. Conceptual representation for the preparation of poly-(1_{0.2}-co-2_{0.8})-MNPs (M = Au and Ag) nanocomposites.

15. TEM images for poly-[(L)-1_r-co-(L)-2_{1-r}]-AuNPs (r = 0.8-0.2) nanocomposites

For TEM studies, a drop of poly-[(L)-1_{0.2}-co-(L)-2_{0.8}]-AuNPs (0.3 mg mL⁻¹) in CHCl₃ was settled onto a carbon film and allowed to dry 12 h. TEM images showed the presence of spherical and low polydisperse AuNPs coating by the helical polymer.

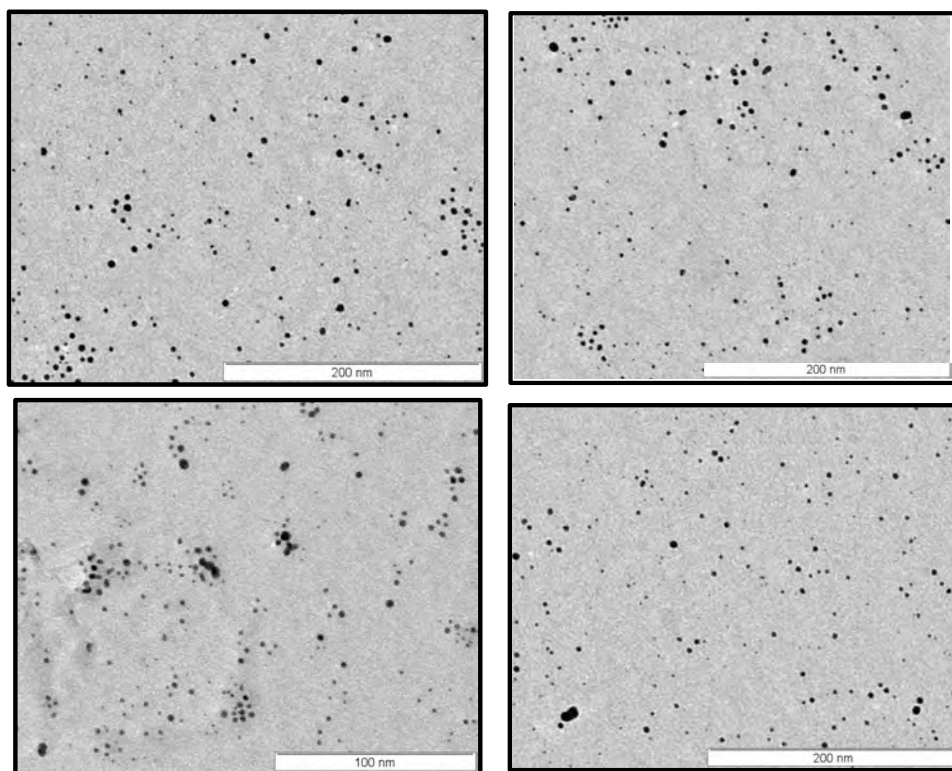


Figure S23. TEM images of poly-[(L)-1_{0.2}-co-(L)-2_{0.8}]-AuNPs.

16. Influence of the amount of AuNPs in the dynamic behaviour of poly-[(L)-1_{0.2}-co-(L)-2_{0.8}]

The influence of the gold nanoparticles (AuNPs) in the secondary structure of poly-[(L)-1_{0.2}-co-(L)-2_{0.8}] was studied by preparation of poly-[(L)-1_{0.2}-co-(L)-2_{0.8}]-AuNPs nanocomposites by addition of different amounts of HAuCl₄ as source of Au³⁺ ions.

For that, a solution of poly-[(L)-1_{0.2}-co-(L)-2_{0.8}] (0.3 mg mL⁻¹) in CHCl₃ was titrated by different amounts of HAuCl₄ (0.2, 0.5, 1.0 and 2.0 equiv., 10 mg mL⁻¹) in MeOH. CD spectra registered for the poly-[(L)-1_{0.2}-co-(L)-2_{0.8}]-AuNPs have shown a decrease in the intensity of the Cotton Effect at 370 nm due to the presence of AuNPs in the polymer chain.

On the other hand, the UV-Vis experiments have shown the typical traces for poly-(**1**_{0.2}-co-**2**_{0.8}) and the LSPR bands have confirmed the formation of AuNPs. Moreover, LSPR bands increase their intensity when the amount of HAuCl₄ is higher.

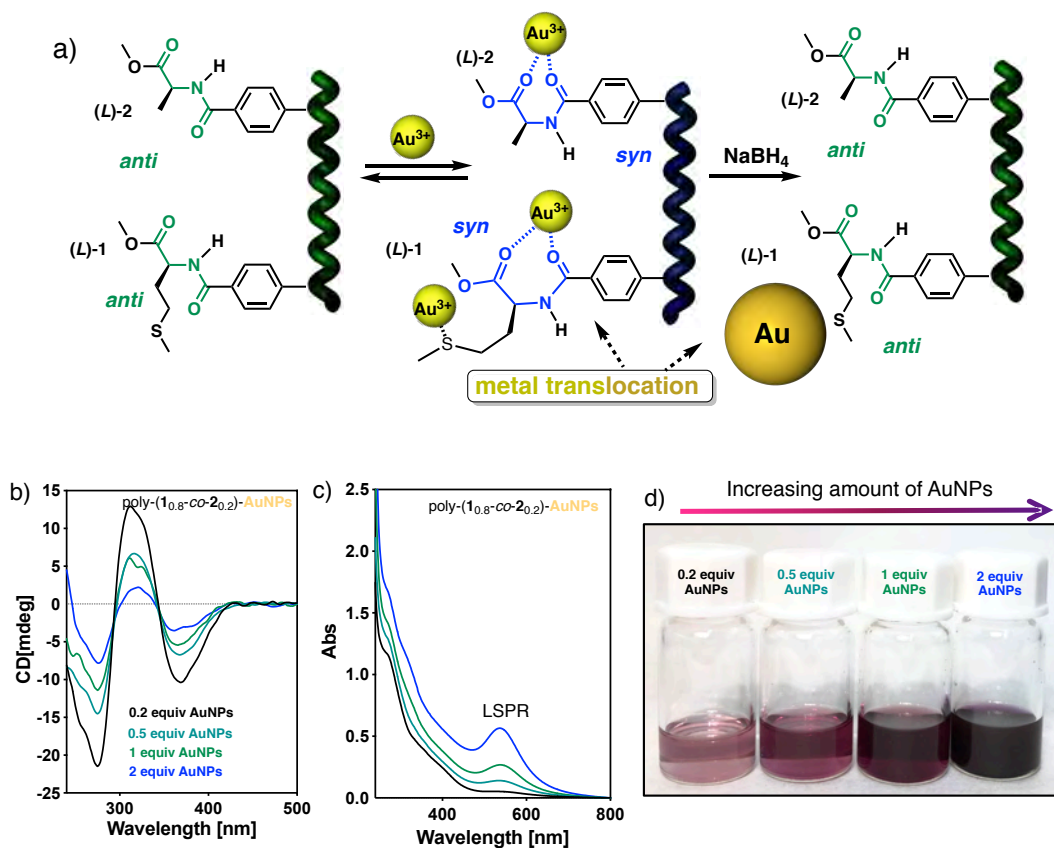


Figure S24. a) Schematic representation for the influence of the AuNPs in the secondary structure of poly-[(L)-**1**_{0.2}-co-(L)-**2**_{0.8}]. b) CD spectra for poly-[(L)-**1**_{0.2}-co-(L)-**2**_{0.8}]-AuNPs with different amount of AuNPs. c) UV-Vis spectra for poly-[(L)-**1**_{0.2}-co-(L)-**2**_{0.8}]-AuNPs with different amount of AuNPs. d) Images for the dispersions of poly-[(L)-**1**_{0.2}-co-(L)-**2**_{0.8}]-AuNPs nanocomposites in CHCl₃.

17. Influence of the amount of AgNPs in the dynamic behaviour of poly-[(L)-**1**_{0.2}-co-(L)-**2**_{0.8}]

The influence of the silver nanoparticles (AgNPs) in the secondary structure of poly-[(L)-**1**_{0.2}-co-(L)-**2**_{0.8}] was studied by preparation of poly-[(L)-**1**_{0.2}-co-(L)-**2**_{0.8}]-AgNPs nanocomposites by addition of different amounts of AgClO₄ as source of Ag⁺ ions.

For that, a solution of poly-[(L)-**1**_{0.2}-co-(L)-**2**_{0.8}] (0.3 mg mL⁻¹) in CHCl₃ was titrated by different amounts of AgClO₄ (0.2, 0.5, 1.0 and 2.0 equiv., 10 mg mL⁻¹) in MeOH. CD spectra registered for the poly-[(L)-**1**_{0.2}-co-(L)-**2**_{0.8}]-AgNPs have shown a decrease in the intensity of the Cotton Effect at 370 nm due to the presence of AgNPs in the PPA chain.

On the other hand, the UV-Vis experiments showed the typical traces for poly-(1_r -co- 2_{1-r}) and the presence of LSPR band confirmed the formation of AgNPs. Moreover, LSPR bands increased their intensity when the amount of AgClO_4 is higher.

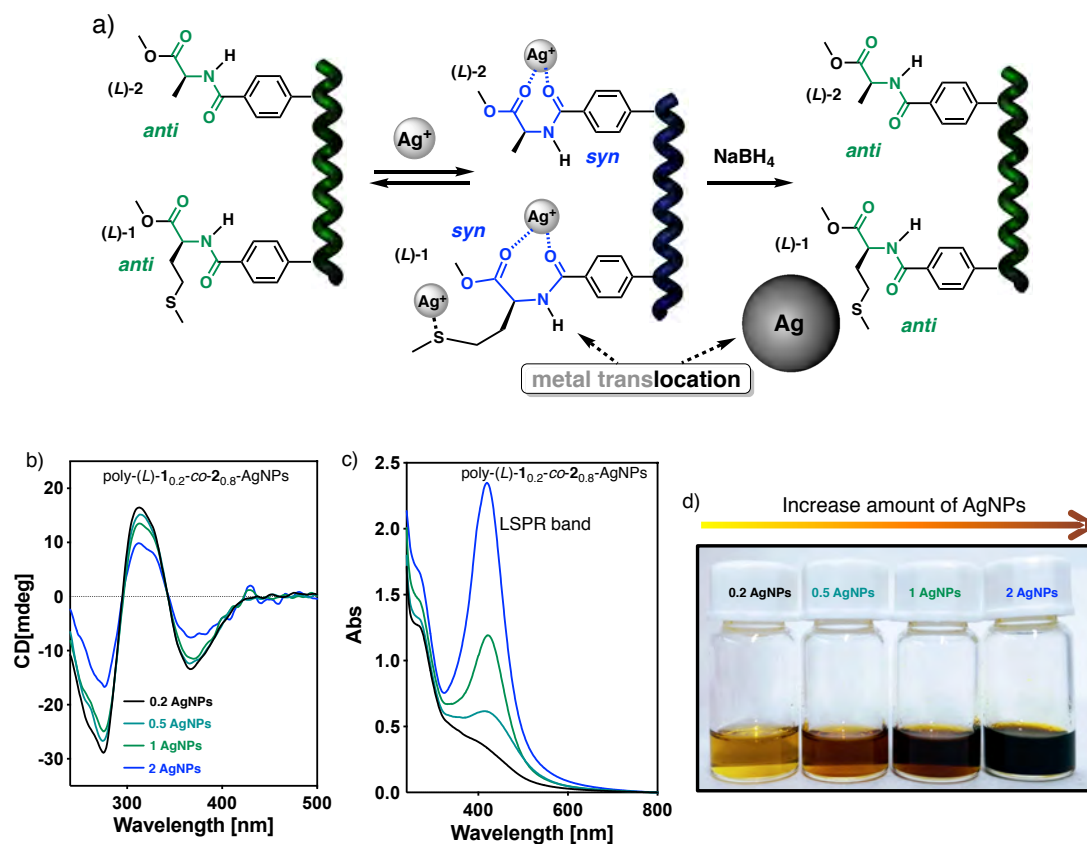


Figure S25. a) Schematic representation for the influence of the AgNPs in the secondary structure of poly-[(L)- $1_{0.2}$ -co-(L)- $2_{0.8}$]. b) CD spectra for poly-[(L)- $1_{0.2}$ -co-(L)- $2_{0.8}$]-AgNPs with different amount of AgNPs. c) UV-Vis spectra for poly-(1_r -co- 2_{1-r})-AgNPs with different amount of AgNPs. d) Images for the dispersions of poly-(1_r -co- 2_{1-r})-AgNPs nanocomposites in CHCl_3 .

18. TEM images for poly-(1_r -co- 2_{1-r})-AgNPs nanocomposites

For TEM studies, a drop of poly-[(L)- $1_{0.2}$ -co-(L)- $2_{0.8}$]-AgNPs (0.3 mg mL^{-1}) in CHCl_3 was settled onto a carbon film and allowed to dry 12 h. TEM images showed the presence of spherical and low polydisperse AgNPs coating by poly-[(L)- $1_{0.2}$ -co-(L)- $2_{0.8}$].

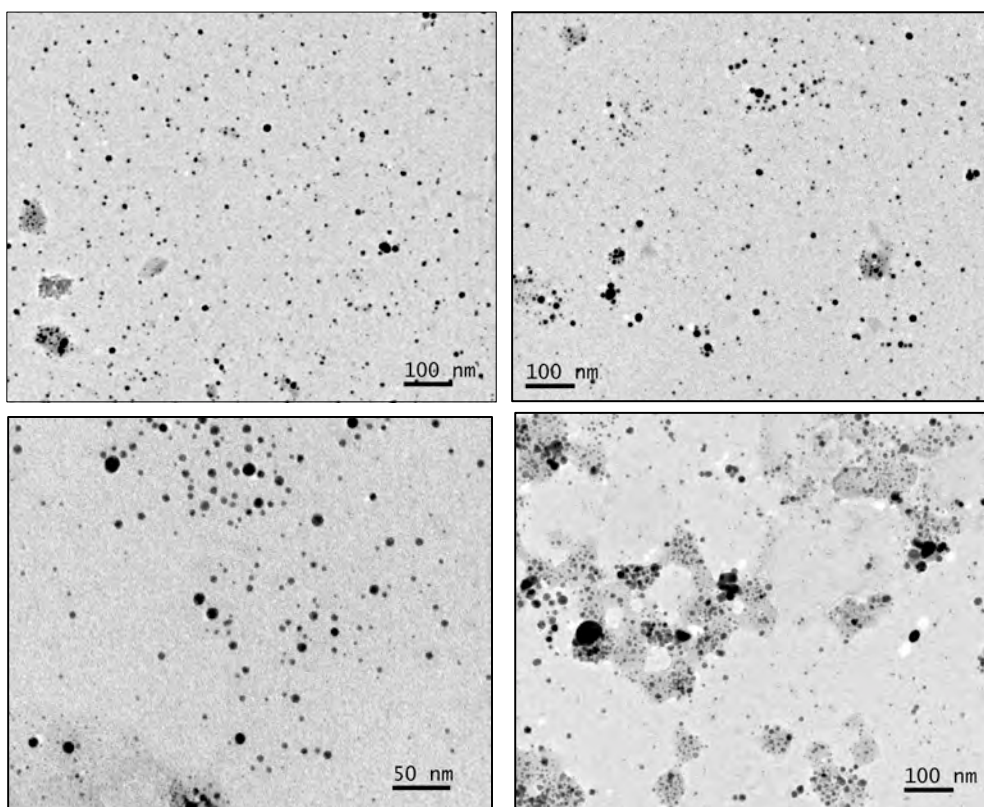


Figure S26. TEM images for poly-[(L)-1_{0.2}-co-(L)-2_{0.8}]-AgNPs.

19. TGA studies of poly-[(L)-1_{0.2}-co-(L)-2_{0.8}]-AuNPs and poly-[(L)-1_{0.2}-co-(L)-2_{0.8}]-AgNPs nanocomposites

TGA Studies were carried out in order to determine the thermal stability of the nanocomposites. As a general protocol, a nanocomposite sample was kept in a platinum pan and heated from 40 °C to 800 °C with a heating rate of 10 °C/min.

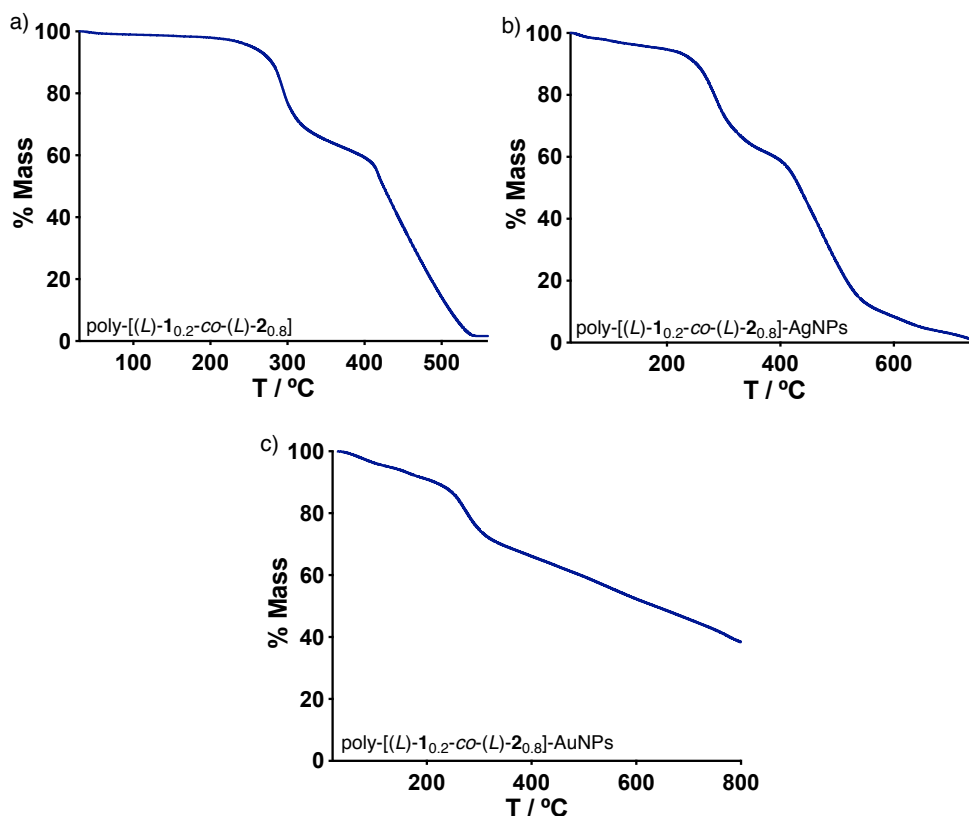


Figure S27. TGA studies for poly-[(L)-1_{0.2}-co-(L)-2_{0.8}], poly-[(L)-1_{0.2}-co-(L)-2_{0.8}]-AgNPs and poly-[(L)-1_{0.2}-co-(L)-2_{0.8}]-AuNPs.

20. Stability studies for poly-[(L)-1_{0.2}-co-(L)-2_{0.8}]-AuNPs nanocomposites

The stability of poly-[(L)-1_{0.2}-co-(L)-2_{0.8}]-AuNPs nanocomposites was determined by CD and UV-Vis measurements at different times.

CD studies for a dispersion of poly-[(L)-1_{0.2}-co-(L)-2_{0.8}]-AuNPs (0.3 mg mL⁻¹) nanocomposites in CHCl₃ at different times have shown the presence of *M* helices (CD₃₇₀ < 0) confirming the stability of the chiral nanocomposites.

UV-Vis measurements for a dispersion of poly-[(L)-1_{0.2}-co-(L)-2_{0.8}]-AuNPs (0.3 mg mL⁻¹) in CHCl₃ have shown the presence of the same LSPR band at different times indicating that the nanocomposites present a good stability in solution.

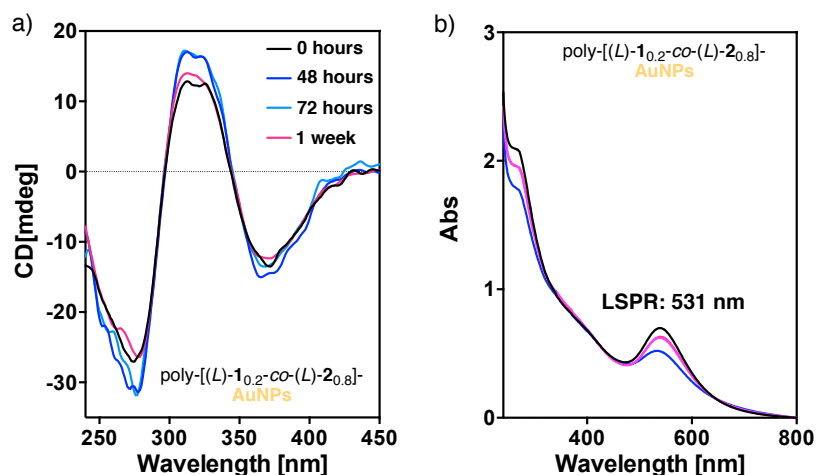


Figure S28. a) CD studies for a dispersion of poly-[(L)-1_{0.2}-co-(L)-2_{0.8}]-AuNPs at different times. b) UV-Vis measurements for a dispersion of poly-[(L)-1_{0.2}-co-(L)-2_{0.8}]-AuNPs at different times.

21. Stability studies for poly-[(L)-1_{0.2}-co-(L)-2_{0.8}]-AgNPs nanocomposites

The stability of poly-[(L)-1_{0.2}-co-(L)-2_{0.8}]-AgNPs nanocomposites was determined by CD and UV-Vis measurements at different times.

CD studies for a dispersion of poly-[(L)-1_{0.2}-co-(L)-2_{0.8}]-AgNPs (0.3 mg mL⁻¹) in CHCl₃ at different times have shown the presence of *M* helices (CD₃₇₀ < 0) indicating that the nanocomposites preserve the helical sense of the parent PPA.

UV-Vis measurements for a dispersion of poly-[(L)-1_{0.2}-co-(L)-2_{0.8}]-AgNPs (0.3 mg mL⁻¹) in CHCl₃ have shown the presence of the same LSPR band at different times indicating that the nanocomposites present a good stability in solution.

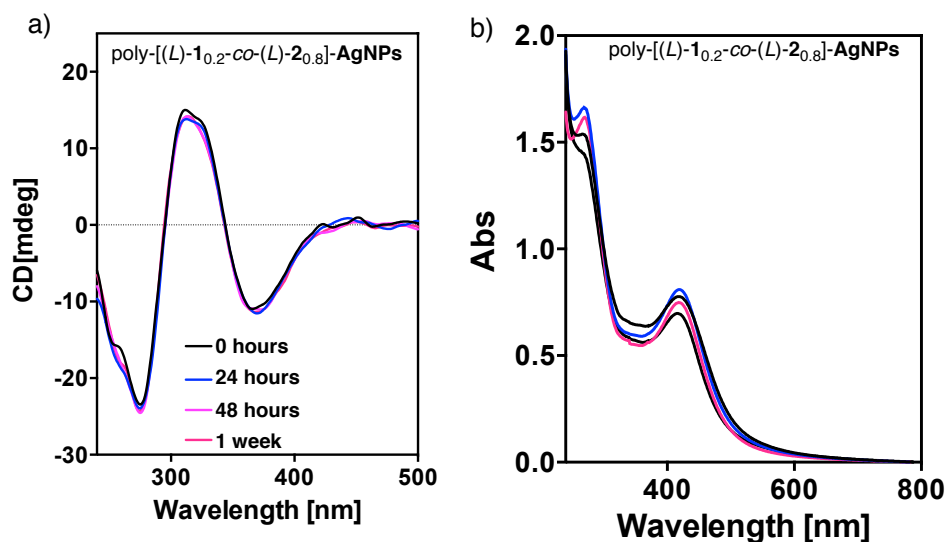
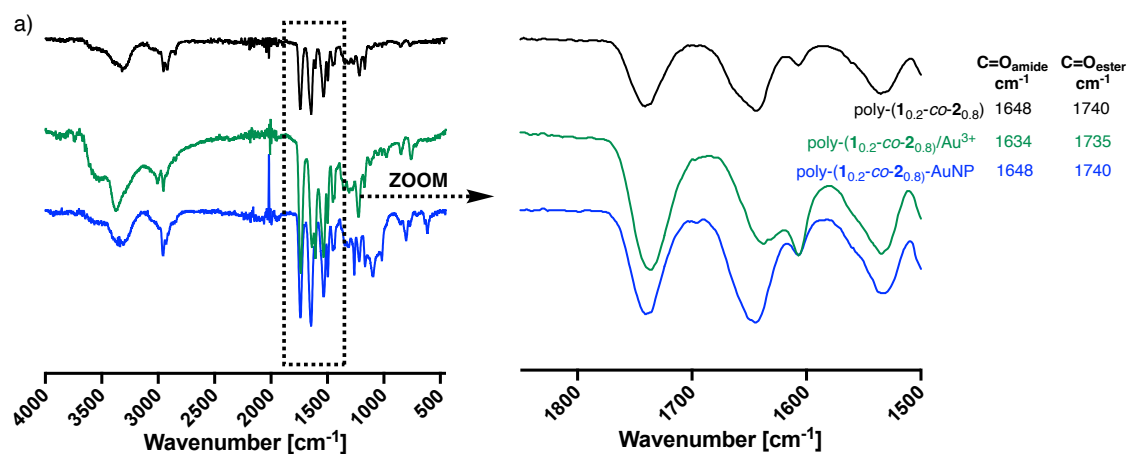


Figure S29. a) CD studies for a dispersion of poly-[(L)-1_{0.2}-co-(L)-2_{0.8}]-AgNPs at different times. b) UV-Vis measurements for a dispersion of poly-[(L)-1_{0.2}-co-(L)-2_{0.8}]-AgNPs a different times.

22. FT-IR experiments for poly-[(L)-1_{0.2}-co-(L)-2_{0.8}]-MNPs (M = Au and/or Ag)

A solution of HAuCl₄ or AgClO₄ (0.5 equiv., 10.0 mg mL⁻¹ in MeOH) was added to a solution of poly-[(L)-1_{0.2}-co-(L)-2_{0.8}]-MNPs (M = Au³⁺ or Ag⁺) (in CHCl₃ (0.3 mg mL⁻¹). Next, NaBH₄ (1 mg mL⁻¹ in MeOH) was added to form poly-[(L)-1_{0.2}-co-(L)-2_{0.8}]-MNPs (M = Au or Ag) nanocomposites and the FT-IR spectra were recorded. The experiments have shown that the nanocomposites present a organic coating formed by poly-[(L)-1_{0.2}-co-(L)-2_{0.8}].



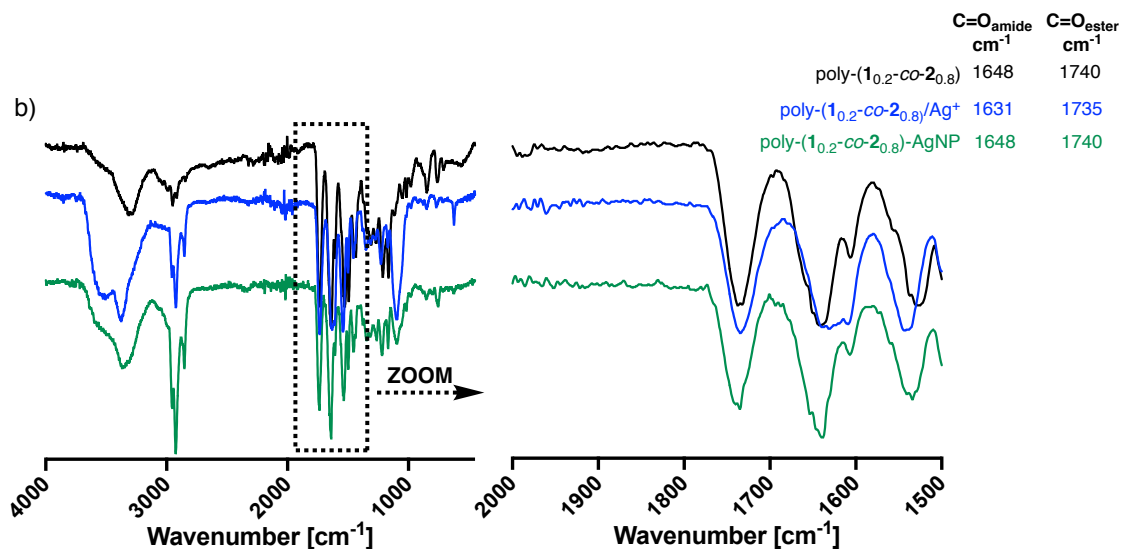
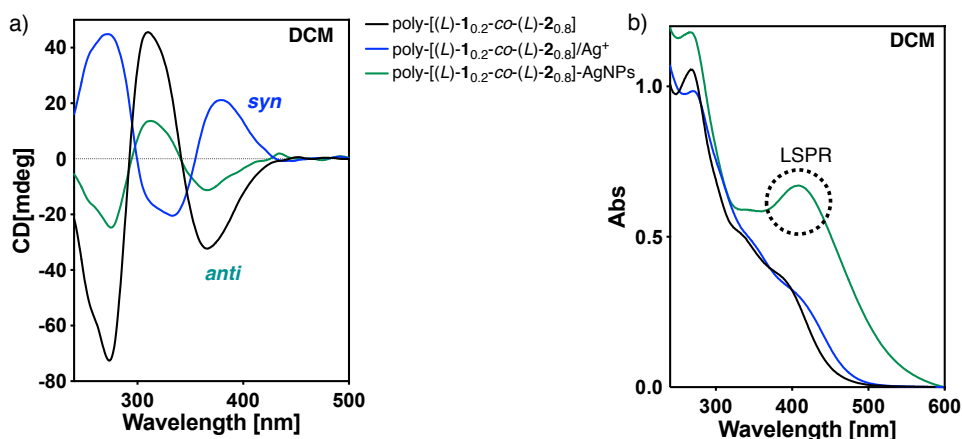


Figure S30. FT experiments for a) poly-(1_r-co-2_{1-r})-AuNPs and b) poly-(1_r-co-2_{1-r})-AgNPs.

23. Stimuli-responsive studies: Preparation of poly-[(L)-1_{0.2}-co-(L)-2_{0.8}]-AgNPs in low polar and high polar solvents

Following the general procedure, poly-[(L)-1_{0.2}-co-(L)-2_{0.8}]-AgNPs nanocomposites were prepared using different high polar (DMSO, DMF) and low-polar (DCM) solvents.

- Preparation of poly-[(L)-1_{0.2}-co-(L)-2_{0.8}]-AgNPs in DCM



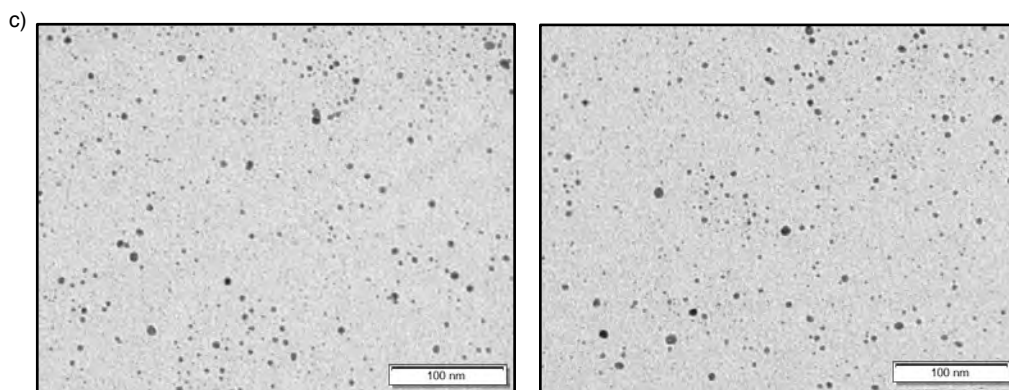


Figure S31. a) CD studies and b) UV-Vis studies of preparation of poly-[(L)-1_{0.2}-co-(L)-2_{0.8}]-AgNPs in and c) poly-[(L)-1_{0.2}-co-(L)-2_{0.8}]-AgNPs in DCM.

- Preparation of poly-[(L)-1_{0.2}-co-(L)-2_{0.8}]-AgNPs in DMF

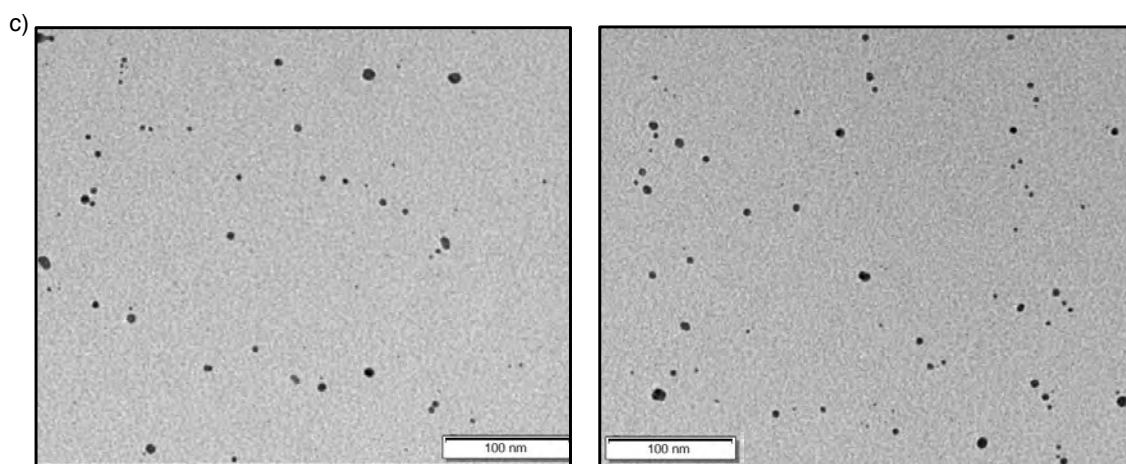
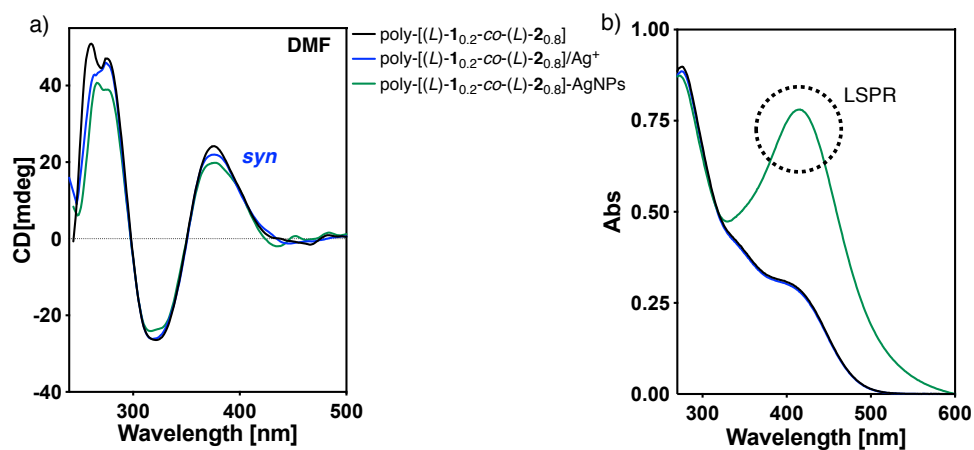


Figure S32. a) CD studies and b) UV-Vis studies of preparation of poly-[(L)-1_{0.2}-co-(L)-2_{0.8}]-AgNPs in and c) TEM images of poly-[(L)-1_{0.2}-co-(L)-2_{0.8}]-AgNPs in DMF.

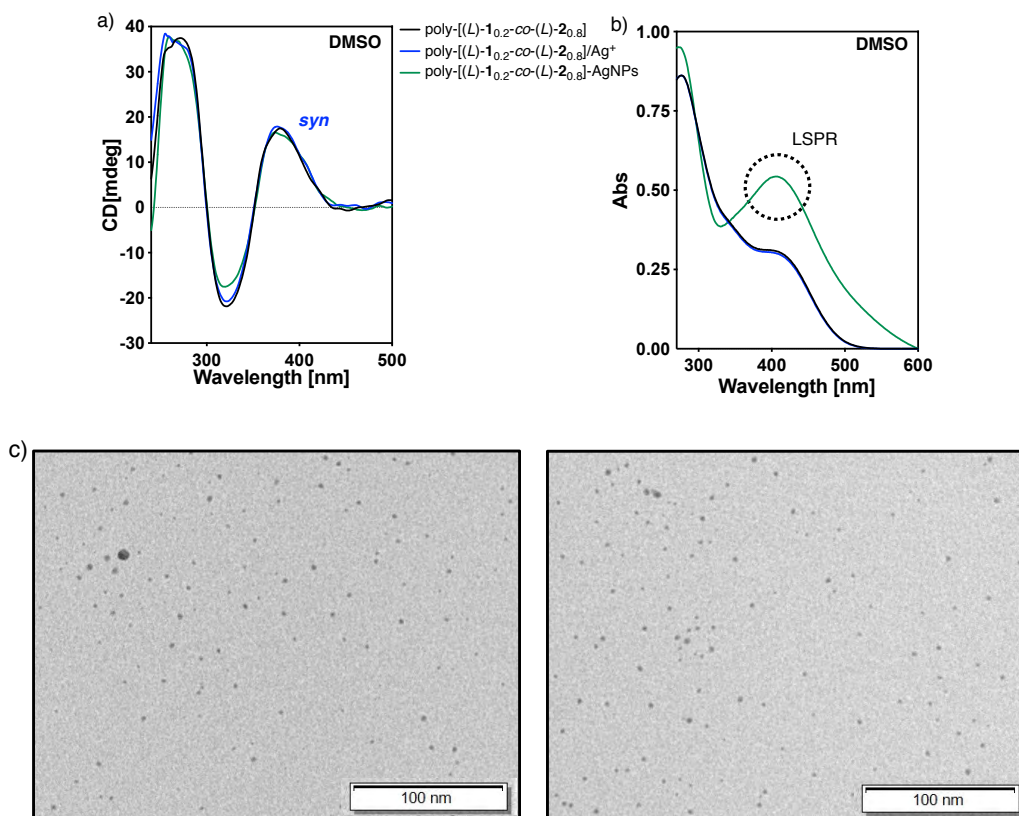


Figure S33. a) CD studies and b) UV-Vis studies of preparation of poly-[(L)-1_{0.2}-co-(L)-2_{0.8}]-AgNPs and c) TEM images of poly-[(L)-1_{0.2}-co-(L)-2_{0.8}]-AgNPs in DMSO.

24. Stimuli-responsive studies: Preparation of poly-[(L)-1_{0.2}-co-(L)-2_{0.8}]-AuNPs in low polar and high polar solvents

Following the general procedure, poly-[(L)-1_{0.2}-co-(L)-2_{0.8}]-AuNPs nanocomposites were prepared using different high polar (DMSO, DMF) and low-polar (DCM) solvents.

- Preparation of poly-[(L)-1_{0.2}-co-(L)-2_{0.8}]-AuNPs in DCM

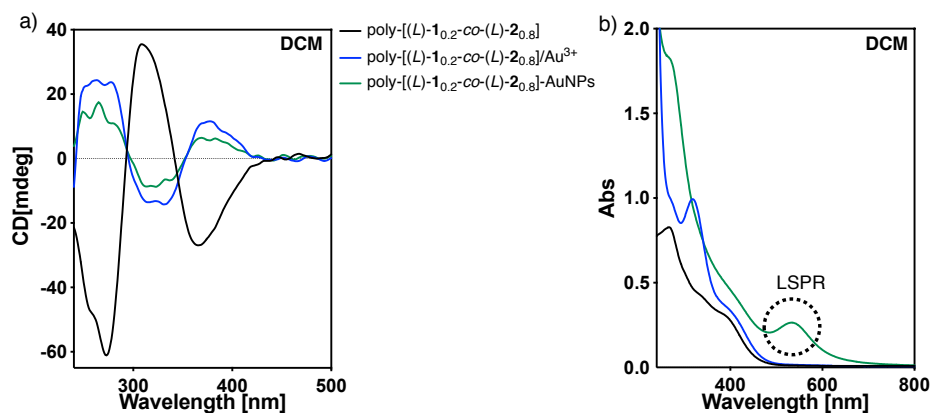


Figure S34. a) CD studies and b) UV-Vis studies of preparation of poly-[(L)-1_{0.2}-co-(L)-2_{0.8}]-AuNPs in DCM.

- Preparation of poly-[(L)-1_{0.2}-co-(L)-2_{0.8}]-AuNPs in DMF

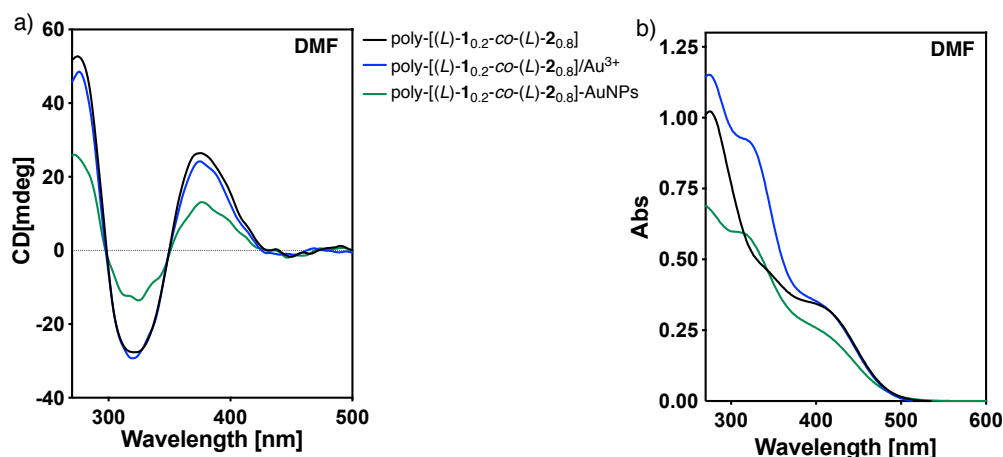


Figure S35. a) CD studies and b) UV-Vis studies of preparation of poly-[(L)-1_{0.2}-co-(L)-2_{0.8}]-AuNPs in DMF.

- Preparation of poly-[(L)-1_{0.2}-co-(L)-2_{0.8}]-AuNPs in DMSO.

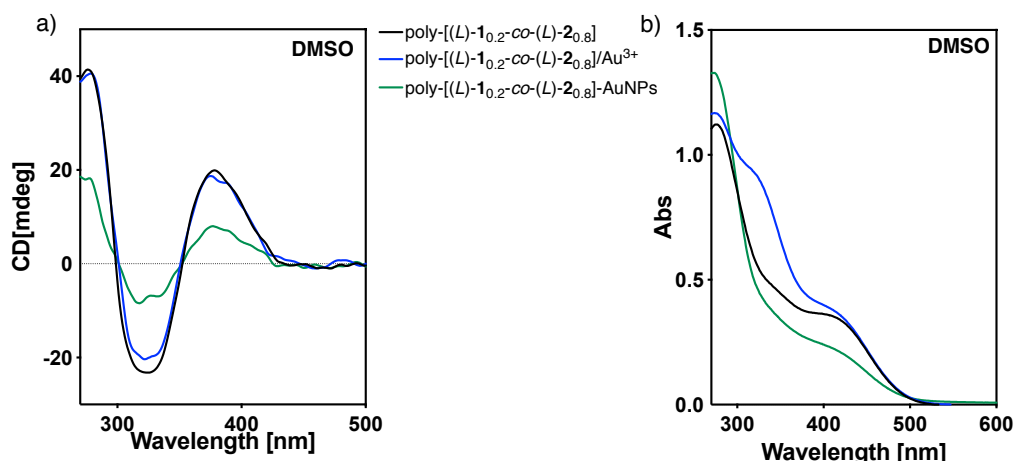


Figure S36. a) CD studies and b) UV-Vis studies of preparation of poly-[(L)-1_{0.2}-co-(L)-2_{0.8}]-AuNPs in DMSO.

25. Control of the helical sense in poly-(1_r-co-2_{1-r})-AgNPs by addition of metal ions

CD studies and UV-Vis were performed with a dispersion of poly-[(L)-1_{0.2}-co-(L)-2_{0.8}]-AgNPs nanocomposites in CHCl₃ (0.3 mg mL⁻¹) using monovalent and divalent metal ions in MeOH (Mⁿ⁺= Li⁺, Ba²⁺) which concentration was 10.0 mg mL⁻¹.

Thus, a dispersion of poly-[(L)-1_{0.2}-co-(L)-2_{0.8}]-AgNPs nanocomposites in CHCl₃ (0.3 mg mL⁻¹) showed the presence of *M* helices (CD₃₇₀ < 0) corresponding to an *anti* conformation between carbonyl groups. The addition of different metal ions (10 mg mL⁻¹

¹, MeOH) promotes a helical inversion ($CD_{370} > 0$) leading to the formation of *P* helices due to the coordination of the M^{n+} ions to both carbonyl groups.

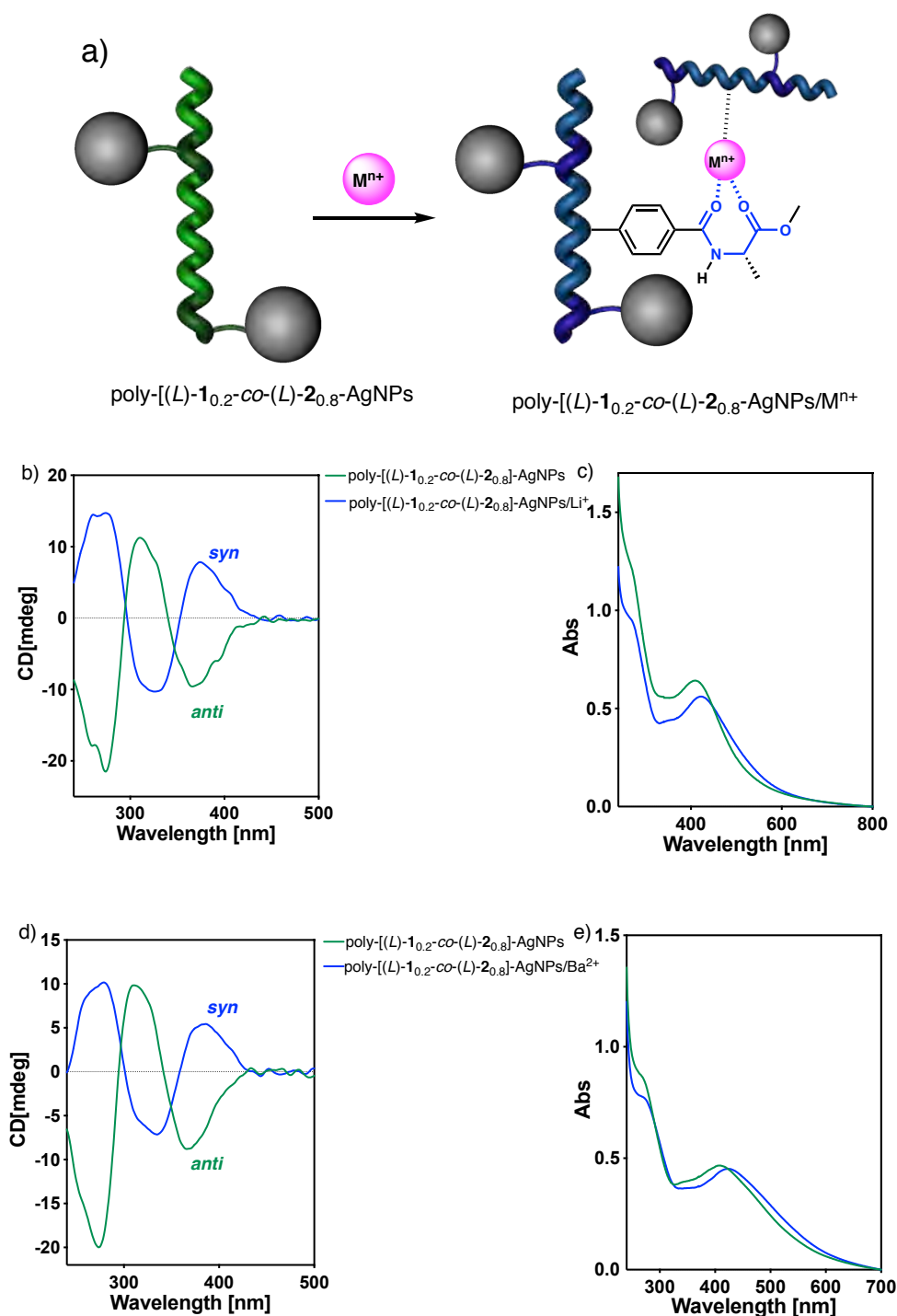


Figure S37. a) Schematic representation of helical sense control in poly-[(L)-1_{0.2}-co-(L)-2_{0.8}]-AgNPs nanocomposites by addition of metal ions. b) CD studies of poly-[(L)-1_{0.2}-co-(L)-2_{0.8}]-AgNPs in presence of Li^+ ions. c) UV-Vis studies of poly-[(L)-1_{0.2}-co-(L)-2_{0.8}]-AgNPs in presence of Li^+ ions. d) CD studies of poly-[(L)-1_{0.2}-co-(L)-2_{0.8}]-AgNPs in presence of Ba^{2+} ions. e) UV-Vis studies of poly-[(L)-1_{0.2}-co-(L)-2_{0.8}]-AuNPs in presence of Ba^{2+} ions.

26. Stimuli-responsive studies: Helical sense control of poly-[(L)-1_{0.2}-co-(L)-2_{0.8}]-AuNPs by addition of metal ions

CD studies and UV-Vis were performed with a dispersion of poly-[(L)-1_{0.2}-co-(L)-2_{0.8}]-AuNPs nanocomposites in CHCl₃ (0.3 mg mL⁻¹) using monovalent and divalent metal ions in MeOH (Mⁿ⁺= Li⁺, Ba²⁺) which concentration was 10.0 mg mL⁻¹.

Thus, a dispersion of poly-[(L)-1_{0.2}-co-(L)-2_{0.8}]-AuNPs nanocomposites in CHCl₃ (0.3 mg mL⁻¹) showed the presence of *M* helices (CD₃₇₀ < 0) corresponding to an *anti* conformation between carbonyl groups. The addition of different metal ions (10 mg mL⁻¹, MeOH) promotes a helical inversion (CD₃₇₀ > 0) leading to the formation of *P* helices due to the coordination of the Mⁿ⁺ ions to both carbonyl groups.

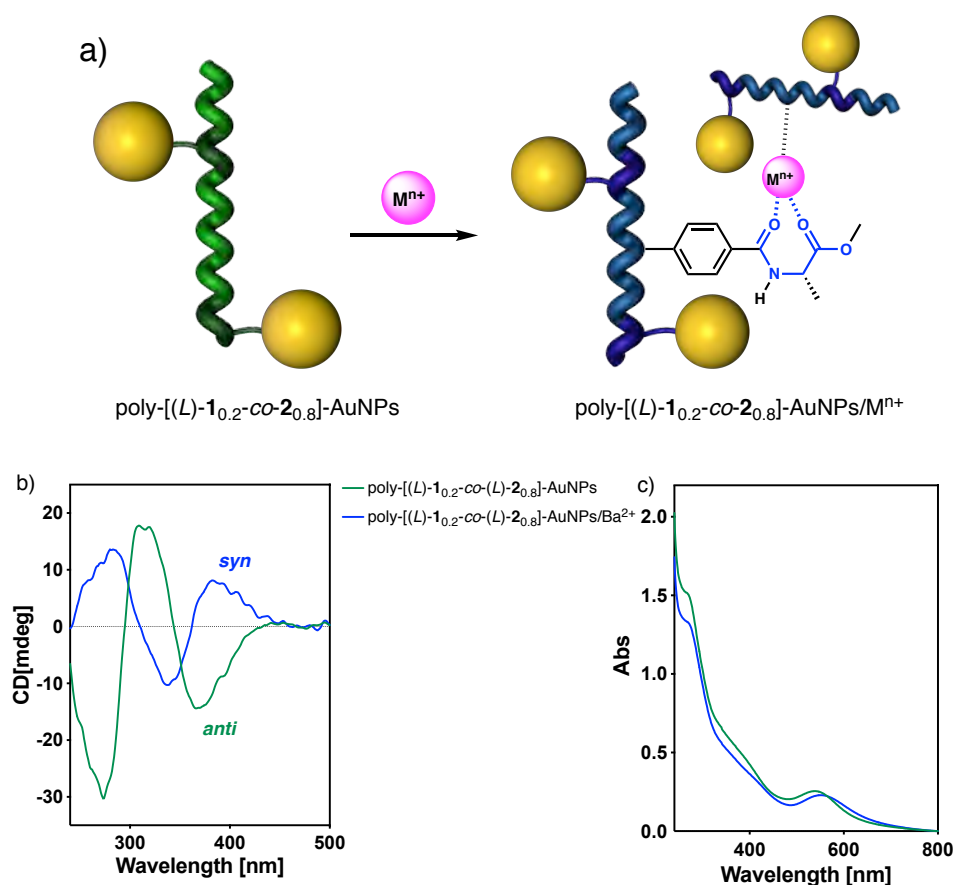


Figure S38. a) Schematic representation of helical sense control in poly-[(L)-1_{0.2}-co-(L)-2_{0.8}]-AuNPs nanocomposites by addition of metal ions. b) CD studies of poly-[(L)-1_{0.2}-co-(L)-2_{0.8}]-AuNPs in presence of Ba²⁺ ions. c) UV-Vis studies of poly-[(L)-1_{0.2}-co-(L)-2_{0.8}]-AuNPs in presence of Ba²⁺ ions.

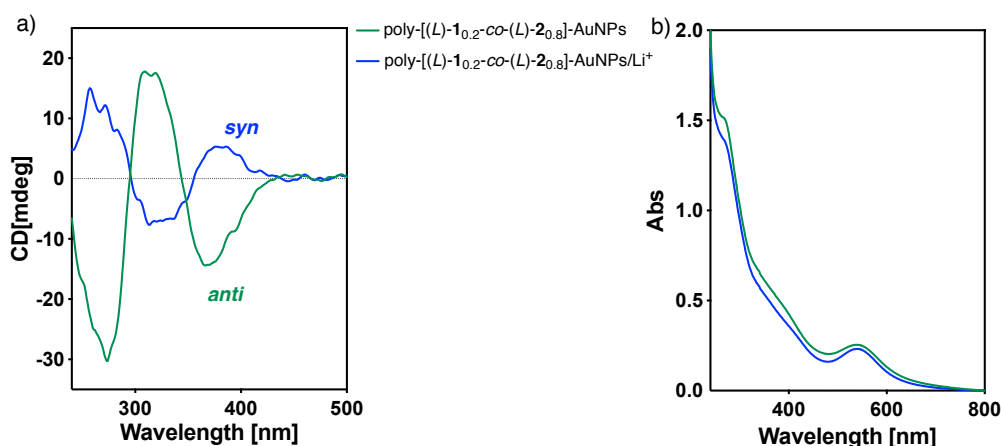


Figure S39. a) CD studies of poly-[(L)-1_{0.2}-co-(L)-2_{0.8}]-AuNPs in presence of Li⁺ ions and b) UV-Vis studies of poly-[(L)-1_{0.2}-co-(L)-2_{0.8}]-AuNPs in presence of Li⁺ ions.

27. SEM images for poly-[(L)-1_{0.2}-co-(L)-2_{0.8}]-AgNPs/Ag⁺ nanospheres

A solution of AgClO₄ (10 mg mL⁻¹, MeOH) was added to a dispersion of poly-[(L)-1_{0.2}-co-(L)-2_{0.8}]-AgNPs or poly-[(L)-1_{0.2}-co-(L)-2_{0.8}]-AuNPs (0.3 mg mL⁻¹, CHCl₃) to form poly-[(L)-1_{0.2}-co-(L)-2_{0.8}]-AgNPs/Ag⁺ or poly-[(L)-1_{0.2}-co-(L)-2_{0.8}]-AuNPs/Ag⁺ complexes. The ability of the Ag⁺ ions to act as crosslinking agents for polymer chains allow forming polymer nanospheres.

DLS studies confirmed the formation of low polydisperse poly-[(L)-1_{0.2}-co-(L)-2_{0.8}]-AgNPs/Ag⁺ or poly-[(L)-1_{0.2}-co-(L)-2_{0.8}]-AuNPs/Ag⁺ nanospheres in solution.

Next, a drop of poly-[(L)-1_{0.2}-co-(L)-2_{0.8}]-AgNPs/Ag⁺ or poly-[(L)-1_{0.2}-co-(L)-2_{0.8}]-AuNPs/Ag⁺ was drop casted onto silicon wafer chip and SEM images were registered.

SEM images obtained have shown the formation of low polydisperse (PDI < 0.2) poly-[(L)-1_{0.2}-co-(L)-2_{0.8}]-AgNPs/Ag⁺ or poly-[(L)-1_{0.2}-co-(L)-2_{0.8}]-AuNPs/Ag⁺ nanospheres. Interestingly, be the presence of AgNPs or AuNPs can be observed on the surface of the nanospheres.

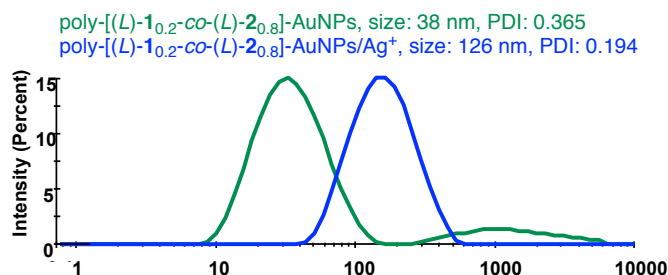


Figure S40. DLS studies of poly-[(L)-1_{0.2}-co-(L)-2_{0.8}]-AuNPs and poly-[(L)-1_{0.2}-co-(L)-2_{0.8}]-AuNPs/Ag⁺ complexes.

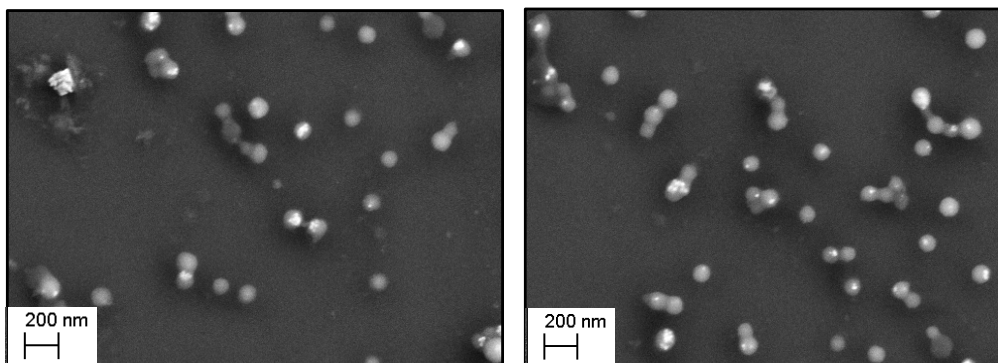


Figure S41. SEM images of poly-[(L)-1_{0.2}-co-(L)-2_{0.8}]-AuNPs/Ag⁺ nanospheres (size: 98 ± 11 nm).

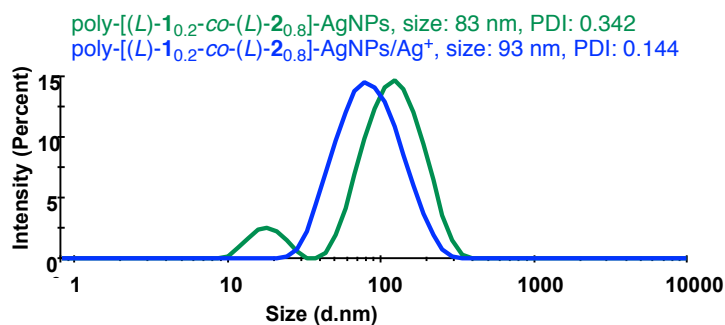


Figure S42. DLS studies of poly-[(L)-1_{0.2}-co-(L)-2_{0.8}]-AgNPs and poly-[(L)-1_{0.2}-co-(L)-2_{0.8}]-AgNPs/Ag⁺ complexes.

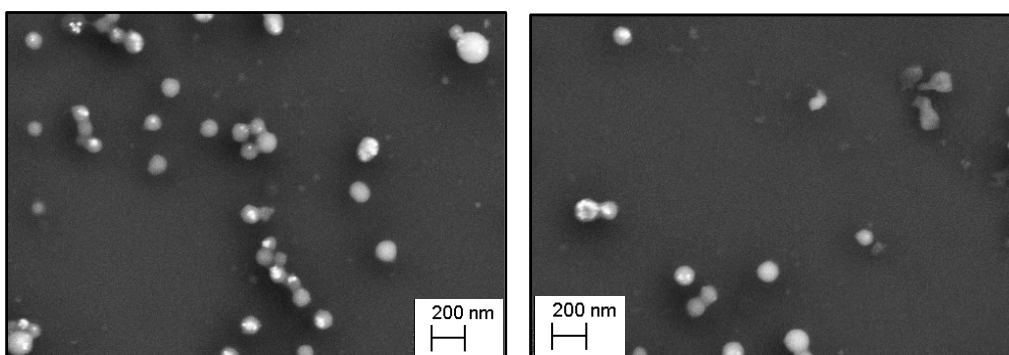
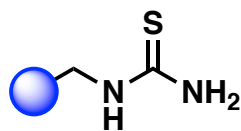


Figure S43. SEM images of poly-[(L)-1_{0.2}-co-(L)-2_{0.8}]-AgNPs/Ag⁺ nanospheres (size: 90 ± 15 nm) nanospheres.

28. Experiments with metal scavenger resins

Commercially available Quadrapure™ (Aldrich) resin (TU) was employed as metal scavenger resin. The TU resin contains a thiourea functional group.



Quadrapure TU

Figure S44. Chemical structure of Quadrapure TU metal scavenger resin.

To carry out these experiments, the resins were swollen in CHCl_3 for 1h (0.05 g mL^{-1}). Next, 100 mg of resins were added to a solution of poly-[(L)-**1**_{0.2}-co-(L)-**2**_{0.8}]-MNPs/ Ag^+ (M = Ag or Au) (0.3 mg mL^{-1} in CHCl_3). After 30 min, CD measurements showed the spectra of poly-[(L)-**1**_{0.2}-co-(L)-**2**_{0.8}]-MNPs ($\text{CD}_{370} < 0$) confirming that Ag^+ ions were removed.

29. Reversibility of the process with resins metal scavengers in presence of silver nanoparticles and metal ions

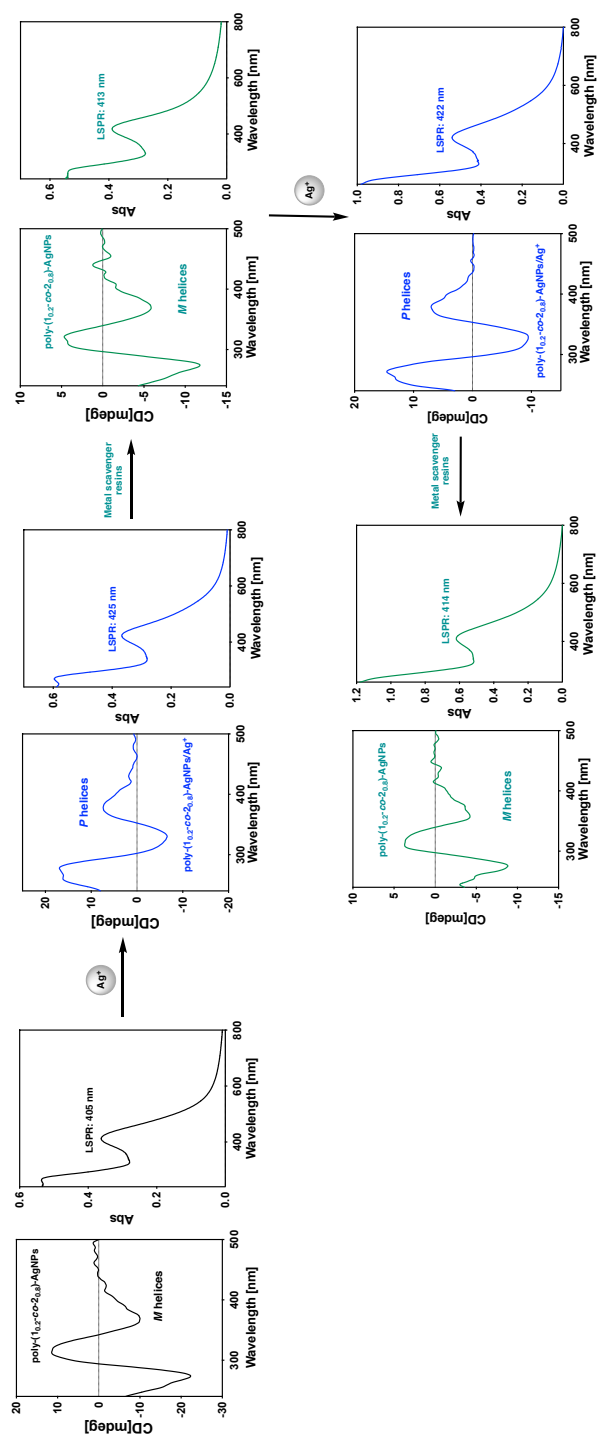


Figure S45. Reversibility process of poly-(1.0.2-co-2.0.8)-AgNPs in presence of Ag⁺ ions.

The use of metal resin scavengers to remove the metal ions (Ag⁺), results also in the loss of a small amount of the nanocomposite, which collapse onto the resin surface.

30. References

[S1] S. Arias, M. Núñez-Martínez, E. Quiñoá, R. Riguera, F. Freire, *Polym. Chem.*, **2017**, 8, 3740-3745.

[S2] J. Bergueiro, M. Núñez-Martínez, S. Arias, E. Quiñoá, R. Riguera, F. Freire, *Nanoscale Horiz.*, **2020**, 5, 495-500.